



Fraunhofer Institut
Techno- und
Wirtschaftsmathematik

N. Marheineke, R. Wegener

Dynamics of curved viscous fibers
with surface tension

© Fraunhofer-Institut für Techno- und Wirtschaftsmathematik ITWM 2007

ISSN 1434-9973

Bericht 115 (2007)

Alle Rechte vorbehalten. Ohne ausdrückliche schriftliche Genehmigung des Herausgebers ist es nicht gestattet, das Buch oder Teile daraus in irgendeiner Form durch Fotokopie, Mikrofilm oder andere Verfahren zu reproduzieren oder in eine für Maschinen, insbesondere Datenverarbeitungsanlagen, verwendbare Sprache zu übertragen. Dasselbe gilt für das Recht der öffentlichen Wiedergabe.

Warennamen werden ohne Gewährleistung der freien Verwendbarkeit benutzt.

Die Veröffentlichungen in der Berichtsreihe des Fraunhofer ITWM können bezogen werden über:

Fraunhofer-Institut für Techno- und
Wirtschaftsmathematik ITWM
Fraunhofer-Platz 1

67663 Kaiserslautern
Germany

Telefon: +49 (0) 6 31/3 16 00-0
Telefax: +49 (0) 6 31/3 16 00-10 99
E-Mail: info@itwm.fraunhofer.de
Internet: www.itwm.fraunhofer.de

Vorwort

Das Tätigkeitsfeld des Fraunhofer-Instituts für Techno- und Wirtschaftsmathematik ITWM umfasst anwendungsnahe Grundlagenforschung, angewandte Forschung sowie Beratung und kundenspezifische Lösungen auf allen Gebieten, die für Techno- und Wirtschaftsmathematik bedeutsam sind.

In der Reihe »Berichte des Fraunhofer ITWM« soll die Arbeit des Instituts kontinuierlich einer interessierten Öffentlichkeit in Industrie, Wirtschaft und Wissenschaft vorgestellt werden. Durch die enge Verzahnung mit dem Fachbereich Mathematik der Universität Kaiserslautern sowie durch zahlreiche Kooperationen mit internationalen Institutionen und Hochschulen in den Bereichen Ausbildung und Forschung ist ein großes Potenzial für Forschungsberichte vorhanden. In die Berichtreihe sollen sowohl hervorragende Diplom- und Projektarbeiten und Dissertationen als auch Forschungsberichte der Institutsmitarbeiter und Institutsgäste zu aktuellen Fragen der Techno- und Wirtschaftsmathematik aufgenommen werden.

Darüber hinaus bietet die Reihe ein Forum für die Berichterstattung über die zahlreichen Kooperationsprojekte des Instituts mit Partnern aus Industrie und Wirtschaft.

Berichterstattung heißt hier Dokumentation des Transfers aktueller Ergebnisse aus mathematischer Forschungs- und Entwicklungsarbeit in industrielle Anwendungen und Softwareprodukte – und umgekehrt, denn Probleme der Praxis generieren neue interessante mathematische Fragestellungen.



Prof. Dr. Dieter Prätzel-Wolters
Institutsleiter

Kaiserslautern, im Juni 2001

Dynamics of Curved Viscous Fibers with Surface Tension

Nicole Marheineke*

Raimund Wegener†

May 31, 2007

Abstract. In this paper we extend the slender body theory for the dynamics of a curved inertial viscous Newtonian fiber [23] by the inclusion of surface tension in the systematic asymptotic framework and the deduction of boundary conditions for the free fiber end, as it occurs in rotational spinning processes of glass fibers. The fiber flow is described by a three-dimensional free boundary value problem in terms of instationary incompressible Navier-Stokes equations under the neglect of temperature dependence. From standard regular expansion techniques in powers of the slenderness parameter we derive asymptotically leading-order balance laws for mass and momentum combining the inner viscous transport with unrestricted motion and shape of the fiber center-line which becomes important in the practical application. For the numerical investigation of the effects due to surface tension, viscosity, gravity and rotation on the fiber behavior we apply a finite volume method with implicit flux discretization.

Keywords. Slender body theory, curved viscous fibers with surface tension, free boundary value problem

AMS Classification. 41A60, 76D05, 35R35, 65N99

1 Introduction

This paper deals with the systematic derivation and numerical investigation of the following asymptotic one-dimensional model for the spinning of a slender curved inertial viscous Newtonian fiber with surface tension. The model determines the dynamics of the fiber center-line γ , the cross-sectional area A , the intrinsic scalar-valued velocity u and the momentum associated vector-valued velocity \mathbf{v} as well as the temporal evolution of the fiber length L for arc-length parameter $s \in [0, L(t))$ and time t :

$$\begin{aligned}\partial_t A + \partial_s(uA) &= 0 \\ \partial_t(A\mathbf{v}) + \partial_s(uA\mathbf{v}) &= \partial_s \left(\left(\frac{3}{\text{Re}} A \partial_s u + \frac{\sqrt{\pi}}{2\text{We}} \right) \partial_s \gamma \right) + A \mathbf{f} \\ \mathbf{v} &= u \partial_s \gamma + \partial_t \gamma\end{aligned}$$

with gravitational and rotational body forces

$$\mathbf{f} = \frac{1}{\text{Fr}^2} \mathbf{e}_g - \frac{2}{\text{Rb}} (\mathbf{e}_\omega \times \mathbf{v}) - \frac{1}{\text{Rb}^2} (\mathbf{e}_\omega \times (\mathbf{e}_\omega \times \gamma))$$

*Technische Universität Kaiserslautern, Fachbereich Mathematik, Postfach 3049, D-67653 Kaiserslautern, nicole@mathematik.uni-kl.de

†Fraunhofer-Institut für Techno- und Wirtschaftsmathematik (ITWM), Fraunhofer-Platz 1, D-67663 Kaiserslautern, wegener@itwm.fhg.de

and the boundary conditions

$$\begin{aligned} \frac{dL(t)}{dt} &= u(L(t), t), \quad L(0) = 0 & (A\partial_s u)(L(t), t) &= \frac{\sqrt{\pi}}{6} \frac{\text{Re}}{\text{We}} \sqrt{A}(L(t), t) \\ A(0, t) &= 1, \quad u(0, t) = 1, \quad \gamma(0, t) = \gamma_0, \quad \partial_s \gamma(0, t) = \tau_0 \end{aligned}$$

at the free fiber end and the nozzle respectively as well as the arc-length parameterization

$$\|\partial_s \gamma\| = 1.$$

Non-dimensionalized with the fluid density, the coefficient of surface tension, the gravitational acceleration, the angular velocity due to the rotation as well as the mean velocity at the nozzle, a typical fiber length and the nozzle area, the model is stated in terms of the dimensionless Reynolds Re , Weber We , Froude Fr and Rossby numbers Rb . The balance laws for mass (cross-section) and momentum are characterized by the two velocities u and \mathbf{v} that are related according to the stated coupling condition: the momentum associated velocity \mathbf{v} is generated by the geometrical motion of the fiber $\partial_t \gamma$ and the intrinsic velocity u that describes the temporal change of the arc-length parameter corresponding to a material point and hence the inner viscous transport. In particular, the balance laws combine the inner viscous transport with the unrestricted motion and shape of the center-line. The form of the model is certainly physically intuitive, but requires the systematic derivation, in particular of the boundary condition at the free end that exclusively depends on the ratio of viscous forces and surface tension. We use the term "unrestricted motion" since we presuppose a highly instationary, curved center-line where $R\kappa \leq 1$ with radius R and curvature κ is allowed. This feature is of great importance for the simulation of rotational spinning processes with highly viscous fluids, see experiments by Wong et.al. [35] and Fig 1.

The understanding of the dynamics of curved viscous inertial fibers with surface tension under gravitation and rotation is generally of interest to research, development and production in the context of glass fiber drawing, tapering and polymer/glass fiber spinning [25]. Our application comes in particular from the glass wool production, cf. Fig 1. In rotational spinning processes, hot molten glass is pressed by centrifugal forces through the perforating walls of a rapidly rotating drum to form thousands of thin curved liquid fibers. These break up into filaments due to the growth of surface tension driven instabilities. These filaments cool and solidify while falling down on a conveyor belt. The theoretical, numerical and experimental investigations of such type of processes cover a wide variety of interesting subjects, i.e. fiber spinning [25, 6, 34], break up behavior and drop forming [11, 24, 35, 31, 32, 19], dynamics and crystallization of non-Newtonian (viscoelastic)

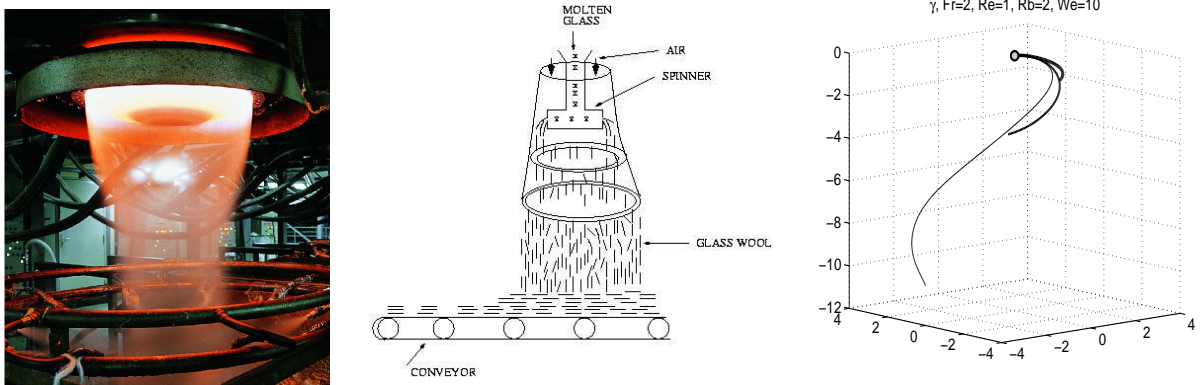


Figure 1: Glass wool production: plant, sketch, simulated fiber motion

flows [14, 13, 1], analysis of instabilities [21, 26, 29, 16, 28, 17, 37, 15], study of effects due to viscosity, surface tension, rotation and gravitation [9, 4, 31, 6, 34], about which a huge amount of literature can be found. In this paper, we focus on the rigorous systematic derivation of the stated one-dimensional model by extending [23] with surface tension and deducing asymptotically appropriate boundary condition for the free end.

For uniaxial flows, such one-dimensional models are well-known in literature and already applied for the theoretical and numerical stability analysis of glass fiber drawing processes, where the boundary condition at the fiber ending is prescribed by the given pulling velocity, e.g. [3, 15, 16, 17, 37]. They have been heuristically derived with and without surface tension from the cross-sectional averaging of the balance laws under certain geometry and profile assumptions, see [12, 26] and references in [8]. Entov et.al. [12] who has incorporated also aerodynamic forces assumes for example a nearly straight center-line, i.e. $R\kappa \ll 1$, $R\lambda \ll 1$ with radius R , curvature κ and torsion λ , circular cross-sections and a given profile-stress distribution. The first systematic derivation approach that forms the basis for several subsequent studies about asymptotic model reductions in this field stems from Dewynne et.al. [8]. This work uses regular asymptotic expansions for the simplification of stationary Stokes flow with instationary free surface, fixed boundaries and without surface tension. Its assumption of a nearly straight center-line has been extended to a curved dynamic center-line in [20]. In addition, an asymptotic fiber model for instationary Navier-Stokes flow with dynamic but nearly straight and at the boundaries given center-line has been deduced in [7] excluding and respectively in [4] including surface tension. The restriction on nearly straight fibers enables the asymptotic analysis in Cartesian coordinates. Numerical investigations of straight Stokes and Navier-Stokes flows without surface tension can be found e.g. in the context of honey dripping under gravity [31, 32]. For curved, coiled flows as they occur in our application, quite heuristic approaches under averaging and stationary assumptions have been stated in [34, 5, 6] and [27]. The works of Decent et.al. [5, 6] deal particularly with the numerical simulation of inviscid and respectively viscous liquid jets from a rotating orifice. A linear stability analysis of spiraling inviscid liquid jets has been developed in [34]. These works presuppose a stationary center-line as well as circular cross-sections and constant velocity profiles in leading order. The curved center-line is handled by a covariant coordinate transformation. For the coiling of viscous jets without surface tension, Ribe [27] proposes an asymptotic analysis that is based on the cross-sectional averaged linear and angular momentum equations together with the assumption of a stationary and moderate curved center-line, i.e. $R\kappa \ll 1$. The uniaxial approaches as well as curved stationary approach by Decent and Wallwork are generalized by Panda's curved, instationary model [23]. Based on the previously derived methodologies, Panda et.al. [23] states a systematic derivation of an asymptotic model for the fiber dynamics without any restrictions on the center-line shape and motion (i.e. $R\kappa \leq 1$), cross-sections, profile quantities nor on the inner viscous transport. To handle the non-linearity and the curved geometry, the formulation of the Navier-Stokes equations in scaled curvilinear coordinates and the splitting of the velocities in the transporting intrinsic u and the transported momentum associated \mathbf{v} are used. However, the neglect of surface tension, $We \rightarrow \infty$, results in a boundary layer in the cross-sections at the free fiber end, i.e. $A(L(t), t) = A(0, 0)$, that is physically unreasonable. Surface tension is a destabilizing mechanism to the flow since its driven instabilities lead to fiber breaking and drop forming, e.g. [11, 24, 35, 30], and to a complex dynamic at the nozzle [5, 34]. Thus, the demand on this paper is the extension of Panda's model by including surface tension and deducing asymptotically appropriate boundary conditions for the free fiber end. So far only heuristic conditions have been suggested e.g. in [11]. The numerical analysis of our final asymptotic model shows a realistic fiber behavior due the effects of viscosity, gravity, rotation and surface tension that coincides with the experiments by Wong et.al. [35].

The three-dimensional free boundary value problem (BVP) for the spinning of a slender curved

inertial viscous fiber is characterized by the slenderness parameter ϵ , i.e. ratio between nozzle diameter and typical fiber length, that is carried into the problem by the inflow and the dynamic boundary conditions due to the definition of the Weber number. Applying the transformation theory of [23] and formulating the free BVP in scaled curvilinear coordinates with respect to the fiber center-line and the slenderness parameter in Sec 2, we embed the BVP into a fiber family whose inflow conditions are independent of ϵ . Their asymptotic analysis in Sec 3 follows the spirit of [8] by using the standard expansion techniques in powers of the slenderness parameter for the model reduction. Thereby we determine the in general unknown relation between the cross-sectional areas and their boundaries by the assumption of radial cross-sections. Comparing the volume averaged three- and one-dimensional balance laws results finally in the appropriate boundary conditions for the free fiber end. The systematically derived one-dimensional fiber model can be understood as generalization of the existing models to the unrestricted dynamic description of a curved viscous fiber with surface tension. The effects of viscosity, gravity, rotation and surface tension on the fiber dynamics are numerically investigated in Sec 4 by applying a finite volume method on a staggered grid with an implicit upwind flux discretization. We particularly examine the unrestricted dynamic fiber description that is important for the practical application.

2 Three-dimensional Model

Consider a single slender curved viscous inertial fiber. Neglecting temperature dependence, the fiber medium is modeled as incompressible Newtonian fluid with surface tension and the fiber spinning as three-dimensional free BVP via incompressible Navier-Stokes equations with free surface and inflow boundary conditions.

2.1 Free Boundary Value Problem

The system of equations is non-dimensionalized by help of the given constant fluid density ρ , the mean velocity at the nozzle V and a fiber length ℓ that is typical in the rotational spinning process. The process is initialized with an empty flow domain at time zero, note that time $t \in \mathbb{R}^+$ in the paper. Let the flow domain at t be denoted by $\Omega^*(t) \subset \mathbb{R}^3$ and its boundary by $\partial\Omega^*(t) = \Gamma_{fr}^*(t) \cup \Gamma_{in}^*$ with $\Gamma_{fr}^*(t) \cap \Gamma_{in}^* = \emptyset$ where $\Gamma_{fr}^*(t)$ and Γ_{in}^* prescribe the time-dependent free surface and the time-independent planar inflow boundary (nozzle), respectively. The small ratio between the nozzle diameter and the fiber length is identified as slenderness parameter ϵ . Due to the scaling with the taken typical velocity V , the dimensionless inflow velocity profile \mathbf{v}_{in} at the nozzle satisfies

$$|\Gamma_{in}^*|^{1/2} = \epsilon \ll 1, \quad (1)$$

$$\int_{\Gamma_{in}^*} \mathbf{v}_{in} \cdot \boldsymbol{\tau}_0 \, d\mathcal{A} = \int_{\Gamma_{in}^*} d\mathcal{A} = \epsilon^2 \quad (2)$$

where $|\Gamma_{in}^*| = \int_{\Gamma_{in}^*} d\mathcal{A}$ is the measure of the cross-sectional area of the nozzle Γ_{in}^* and $\boldsymbol{\tau}_0$ its inner normal vector. The process is characterized by the dimensionless Reynolds $\text{Re} = \ell\rho V/\mu$ and Weber numbers $\text{We} = (\epsilon\ell/2)\rho V^2/\sigma$ with dynamic viscosity μ and coefficient of surface tension σ . The chosen length $\epsilon\ell/2$ in the Weber number can be understood as the typical radius of curvature of the free surface.

Then, the model for the free BVP reads

Balance laws, $\mathbf{r} \in \Omega^(t)$*

$$\begin{aligned} \nabla_{\mathbf{r}} \cdot \mathbf{v}(\mathbf{r}, t) &= 0 \\ \partial_t \mathbf{v}(\mathbf{r}, t) + \nabla_{\mathbf{r}} \cdot (\mathbf{v} \otimes \mathbf{v})(\mathbf{r}, t) &= \nabla_{\mathbf{r}} \cdot \mathbf{T}^T(\mathbf{r}, t) + \mathbf{f}(\mathbf{r}, t) \end{aligned}$$

Constitutive law

$$\mathbf{T} = -p\mathbf{I} + \frac{1}{\text{Re}}(\nabla_{\mathbf{r}}\mathbf{v} + (\nabla_{\mathbf{r}}\mathbf{v})^T)$$

Kinematic and dynamic boundary conditions, $\mathbf{r} \in \Gamma_{fr}^(t)$*

$$(\mathbf{v} \cdot \mathbf{n}^*)(\mathbf{r}, t) = w^*(\mathbf{r}, t), \quad (\mathbf{T} \cdot \mathbf{n}^*)(\mathbf{r}, t) = -\frac{\epsilon}{\text{We}}(H\mathbf{n}^*)(\mathbf{r}, t)$$

Inflow boundary condition, $\mathbf{r} \in \Gamma_{in}^$*

$$\mathbf{v}(\mathbf{r}, t) = \mathbf{v}_{in}(\mathbf{r})$$

Initial condition

$$\Omega^*(0) = \emptyset$$

The unknowns of the BVP are the field variables for velocity \mathbf{v} and pressure p as well as the geometry of the flow domain that is determined by the unit outer normal vectors \mathbf{n}^* and the scalar speed w^* of the free surface $\Gamma_{fr}^*(t)$. The jump in the normal stresses at $\Gamma_{fr}^*(t)$ is incorporated in the definition of the stress tensor \mathbf{T} by choosing p as hydrodynamic pressure being relative with regard to the constant atmospheric one. Then, the inhomogeneous dynamic boundary condition for \mathbf{T} where the mean curvature H is deduced from the geometry include the effects of surface tension in the model. The appropriate choice of body forces \mathbf{f} completes the model, e.g. gravitational and rotational forces are considered.

2.2 Coordinate Transformations

Following the systematic asymptotic concept of [23] for the model reduction, the free BVP is transformed into general coordinates being specified as scaled curvilinear. These coordinates can be understood as generalization of cylindrical ones along an arbitrary curve with which the fiber center-line is associated. The scaling leads to inflow conditions independent of the slenderness parameter. Hence, after briefly stating the basic theory of the coordinate transformation [23], the free BVP in scaled curvilinear coordinates is embedded into a family of self-similar problems with fixed inflow domain and fixed inflow velocity.

Definition 1 (Time-dependent General Coordinate Transformation) *A function $\check{\mathbf{r}}$ defined by $\check{\mathbf{r}}(\cdot, t): \Omega(t) \subset \mathbb{R}^3 \mapsto \Omega^*(t) \subset \mathbb{R}^3$ for $t \in \mathbb{R}^+$ is called time-dependent general coordinate transformation if $\check{\mathbf{r}} \in \mathcal{C}^2$ and if its restrictions $\check{\mathbf{r}}(\cdot, t)$ are bijective.*

The function $\check{\mathbf{r}}$ maps chosen time-dependent coordinates \mathbf{x} onto a spatial point \mathbf{r} , whereas $\check{\mathbf{x}}$ maps any point onto its coordinates. Consequently, scalar, vector and tensor fields can be defined in spatial points or general coordinates, i.e. $\tilde{f}(\mathbf{x}, t) = f(\check{\mathbf{r}}(\mathbf{x}, t), t)$ and $f(\mathbf{r}, t) = \tilde{f}(\check{\mathbf{x}}(\mathbf{r}, t), t)$. In the following we suppress the distinction by tilde to keep the terminology simple. Related to a given $\check{\mathbf{r}}$ the following characteristic quantities are introduced:

- Inverse mapping $\check{\mathbf{r}}(\check{\mathbf{x}}(\mathbf{r}, t), t) = \mathbf{r}$ and $\check{\mathbf{x}}(\check{\mathbf{r}}(\mathbf{x}, t), t) = \mathbf{x}$
- Coordinate transformation matrix $\mathbf{F}(\mathbf{x}, t) = \nabla_{\mathbf{x}}\check{\mathbf{r}}(\mathbf{x}, t)$
- Functional determinant $J(\mathbf{x}, t) = \det(\mathbf{F}(\mathbf{x}, t))$
- Inverse matrix $\mathbf{G}(\mathbf{x}, t) = \mathbf{F}^{-1}(\mathbf{x}, t) = \nabla_{\mathbf{r}}\check{\mathbf{x}}(\check{\mathbf{r}}(\mathbf{x}, t), t)$
- Coordinate velocity $\mathbf{q}(\mathbf{x}, t) = \partial_t\check{\mathbf{r}}(\mathbf{x}, t)$

Definition 2 (Transformation of Observables) *For the observables of the free BVP the following transformed fields in general coordinates are introduced*

- *Stress tensor* $\mathbf{S}(\mathbf{x}, t) = J(\mathbf{x}, t) \mathbf{T}(\mathbf{x}, t) \cdot \mathbf{G}(\mathbf{x}, t)$
- *Intrinsic velocity* $\mathbf{u}(\mathbf{x}, t) = (\mathbf{v}(\mathbf{x}, t) - \mathbf{q}(\mathbf{x}, t)) \cdot \mathbf{G}(\mathbf{x}, t)$
- *Normal vectors* $\mathbf{n}(\mathbf{x}, t) = \frac{\mathbf{F} \cdot \mathbf{n}^*}{\|\mathbf{F} \cdot \mathbf{n}^*\|}(\mathbf{x}, t)$
- *Surface speed* $w(\mathbf{x}, t) = \frac{(w^* - \mathbf{q} \cdot \mathbf{n}^*)}{\|\mathbf{F} \cdot \mathbf{n}^*\|}(\mathbf{x}, t)$

The transformations in Def 2 keep the physical and geometrical properties of the observables and enable the formulation of the free BVP in general coordinates in terms of balance laws where the functional determinant J represents the density. The relation of the two introduced velocities, \mathbf{u} and \mathbf{v} is expressed in the coupling condition: the intrinsic velocity \mathbf{u} describes the convection/transport of the unknowns in the balance laws, whereas the momentum associated velocity \mathbf{v} represents the transported quantity. The derivation of the BVP is sketched in [23] for homogeneous dynamic boundary conditions. The stated inhomogeneous dynamic boundary conditions result directly from Def 2. Thereby, H prescribes the mean curvature of the spatial geometry $\Omega^*(t)$ at points that are addressed by the general coordinates.

Balance laws, $\mathbf{x} \in \Omega(t)$

$$\begin{aligned} \partial_t J(\mathbf{x}, t) + \nabla_{\mathbf{x}} \cdot (J\mathbf{u})(\mathbf{x}, t) &= 0 \\ \partial_t (J\mathbf{v})(\mathbf{x}, t) + \nabla_{\mathbf{x}} \cdot (\mathbf{u} \otimes J\mathbf{v})(\mathbf{x}, t) &= \nabla_{\mathbf{x}} \cdot \mathbf{S}^T(\mathbf{x}, t) + (J\mathbf{f})(\mathbf{x}, t) \end{aligned}$$

Coupling condition

$$\mathbf{u} = (\mathbf{v} - \mathbf{q}) \cdot \mathbf{G}$$

Constitutive law

$$\mathbf{S} = J \left(-p \mathbf{I} + \frac{1}{\text{Re}} ((\mathbf{G} \cdot \nabla \mathbf{v}) + (\mathbf{G} \cdot \nabla \mathbf{v})^T) \right) \cdot \mathbf{G}$$

Kinematic and dynamic boundary conditions, $\mathbf{x} \in \Gamma_{fr}(t)$

$$(\mathbf{u} \cdot \mathbf{n})(\mathbf{x}, t) = w(\mathbf{x}, t), \quad (\mathbf{S} \cdot \mathbf{n})(\mathbf{x}, t) = -\frac{\epsilon}{\text{We}} (JH\mathbf{G} \cdot \mathbf{n})(\mathbf{x}, t)$$

Inflow boundary condition, $\mathbf{x} \in \Gamma_{in}$

$$\mathbf{v}(\mathbf{x}, t) = \mathbf{v}_{in}(\mathbf{x})$$

Initial condition

$$\Omega(0) = \emptyset$$

To specify the general coordinates as scaled curvilinear ones, a three-dimensional time-dependent curve $\gamma(s, t)$ in the domain $\Omega(t) \subset \mathbb{R}^3$ is introduced that is parameterized with respect to the arc-length $s \in \mathbb{R}_0^+$. Assuming sufficient regularity of γ , curvature $\kappa = \|\partial_{ss}\gamma\|$, $\kappa \neq 0$ and torsion $\lambda = \partial_s \gamma \cdot (\partial_{ss}\gamma \times \partial_{sss}\gamma)/\kappa^2$ are well-defined. Define a orthonormal basis corresponding to γ by

$$\boldsymbol{\tau} = \partial_s \gamma, \quad \boldsymbol{\eta}_1 = \cos(\phi)\boldsymbol{\eta} - \sin(\phi)\mathbf{b}, \quad \boldsymbol{\eta}_2 = \sin(\phi)\boldsymbol{\eta} + \cos(\phi)\mathbf{b}$$

with the tangent $\boldsymbol{\tau}$, normal $\boldsymbol{\eta} = \partial_{ss}\gamma/\kappa$ and binormal vectors $\mathbf{b} = \boldsymbol{\tau} \times \boldsymbol{\eta}$ as well as the torsion angle $\phi(s, t) = \int_0^s \lambda(\sigma, t) d\sigma$, [2]. Based on the Serret-Frenet formulae their relations are formulated as

$$\partial_s \boldsymbol{\tau} = (\partial_\alpha h)\boldsymbol{\eta}_\alpha, \quad \partial_s \boldsymbol{\eta}_\alpha = -(\partial_\alpha h)\boldsymbol{\tau} \quad \text{with } h(\mathbf{x}, t) = x_1 \kappa \cos(\phi) + x_2 \kappa \sin(\phi), \quad \alpha = 1, 2.$$

Note that we apply the generalized Einstein summation convention in this paper. Latin indices have values out of the set $\{1, 2, 3\}$, Greek indices out of $\{1, 2\}$.

Definition 3 (Scaled Curvilinear Coordinate Transformation) For a given arc-length parameterized and smooth curve γ and a fixed parameter $\epsilon \in \mathbb{R}^+$ the special choice of a time-dependent general coordinate transformation

$$\check{\mathbf{r}}(\mathbf{x}, t) = \gamma(s, t) + \epsilon x_1 \boldsymbol{\eta}_1(s, t) + \epsilon x_2 \boldsymbol{\eta}_2(s, t) \quad \text{with} \quad s = x_3$$

is called scaled curvilinear coordinate transformation, if $\check{\mathbf{r}}(\cdot, t)$ is bijective for $t \in \mathbb{R}^+$.

Using the canonical basis $\mathbf{e}_i, i = 1, 2, 3$ in \mathbb{R}^3 , the characteristic quantities of a scaled curvilinear coordinate transformation read

- Coordinate transformation matrix $\mathbf{F} = \mathbf{e}_i \otimes \mathbf{f}_i, \mathbf{f}_1 = \epsilon \boldsymbol{\eta}_1, \mathbf{f}_2 = \epsilon \boldsymbol{\eta}_2, \mathbf{f}_3 = (1 - \epsilon h) \boldsymbol{\tau}$
- Functional determinant $J = \epsilon^2 (1 - \epsilon h)$
- Inverse matrix $\mathbf{G} = \mathbf{g}_i \otimes \mathbf{e}_i, \mathbf{g}_1 = \frac{1}{\epsilon} \boldsymbol{\eta}_1, \mathbf{g}_2 = \frac{1}{\epsilon} \boldsymbol{\eta}_2, \mathbf{g}_3 = \frac{1}{(1 - \epsilon h)} \boldsymbol{\tau}$
- Coordinate velocity $\mathbf{q} = \partial_t \gamma + \epsilon x_\alpha \partial_t \boldsymbol{\eta}_\alpha$

This yields the representation of the Newtonian stress tensor \mathbf{S} in scaled curvilinear coordinates, [23, 22], where $u_i := \mathbf{u} \cdot \mathbf{e}_i, i = 1, 2, 3$

$$\begin{aligned} \mathbf{S} = & -p \left(\epsilon(1 - \epsilon h) (\boldsymbol{\eta}_\alpha \otimes \mathbf{e}_\alpha) + \epsilon^2 (\boldsymbol{\tau} \otimes \mathbf{e}_3) \right) \\ & + \frac{1}{\text{Re}} \left(\epsilon(1 - \epsilon h) (\partial_\alpha u_\beta + \partial_\beta u_\alpha) (\boldsymbol{\eta}_\alpha \otimes \mathbf{e}_\beta) + (\epsilon(1 - \epsilon h) \partial_\alpha u_3 + \frac{\epsilon^3}{(1 - \epsilon h)} \partial_s u_\alpha) (\boldsymbol{\eta}_\alpha \otimes \mathbf{e}_3) \right. \\ & \left. + (\epsilon^2 \partial_s u_\alpha + (1 - \epsilon h)^2 \partial_\alpha u_3) (\boldsymbol{\tau} \otimes \mathbf{e}_\alpha) + (2\epsilon^2 \partial_s u_3 + \frac{2\epsilon^3}{(1 - \epsilon h)} h (\partial_\alpha u_\alpha + \partial_s u_3)) (\boldsymbol{\tau} \otimes \mathbf{e}_3) \right) \end{aligned}$$

2.3 Fiber Family in Scaled Curvilinear Coordinates

Applying the scaled curvilinear coordinate transformation on our fiber problem, its representative quantities, i.e. the curve γ and the scaling factor ϵ , are specified by the center-line of the fiber and the slenderness parameter in Eq (1). This choice has some crucial consequences for the logical structure of our problem. Since the dynamics of the center-line depends on the solution of the free BVP, the coordinate transformation becomes part of the problem. Therefore, we impose the following assumption of [23] concerning the fiber domain and its cross-sections.

Assumption 4 (Fiber Geometry) Let $\Omega^*(t)$ be the flow domain of the fiber spinning process and ϵ the slenderness parameter of Eq (1). Moreover, let $\gamma(\cdot, t): [0, L(t)) \mapsto \Omega^*(t)$ for $t \in \mathbb{R}^+$ be a time-dependent arc-length parameterized curve. Then, assume

- A scaled curvilinear coordinate transformation $\check{\mathbf{r}}(\cdot, t): \Omega(t) \mapsto \Omega^*(t)$ for $t \in \mathbb{R}^+$ exists with respect to ϵ and γ .
- $\Omega(t)$ is given by the fiber length $L(t)$ and the smooth, 2π -periodic radius function $R(\cdot, t): [0, 2\pi) \times [0, L(t)) \mapsto \mathbb{R}^+$ in such a way that

$$\Omega(t) = \{ \mathbf{x} = (x_1, x_2, s) \in \mathbb{R}^3 \mid (x_1, x_2) \in \mathcal{A}(s, t), s \in [0, L(t)) \}$$

with cross-sections

$$\mathcal{A}(s, t) = \{ (x_1, x_2) \in \mathbb{R}^2 \mid x_1 = \varrho \cos(\psi), x_2 = \varrho \sin(\psi), \varrho \in [0, R(\psi, s, t)], \psi \in [0, 2\pi) \}.$$

- The curve γ satisfies the center-line condition, i.e.

$$\int_{\mathcal{A}(s,t)} x_1 dx_1 dx_2 = \int_{\mathcal{A}(s,t)} x_2 dx_1 dx_2 = 0.$$

The assumption answers the question of the validity of the asymptotic result. This depends on the bijectivity of the coordinate transformation and is hurt if $R\kappa > 1$. This constraint is obviously weaker than the assumption $R\kappa \ll 1$, e.g. used in [12, 27]. The whole fiber domain in the scaled curvilinear coordinates is completely described by the three quantities: fiber length L , center-line γ and radius function R . As consequence, the fiber geometry has a bottom surface that might shrink to a single point, $|\mathcal{A}(L(t), t)| = 0$, due to the acting surface tension. Hence, we distinguish between the lateral and the bottom surface of the free surface, i.e. $\Gamma_{fr}(t) = \Gamma_{lat}(t) \cup \Gamma_{bot}(t)$, $\Gamma_{lat}(t) \cap \Gamma_{bot}(t) = \emptyset$.

The lateral surface $\Gamma_{lat}(t)$ can be parameterized by the bijective function $\boldsymbol{\xi}(\cdot, t): [0, 2\pi) \times [0, L(t)) \mapsto \Gamma_{lat}(t) \subset \mathbb{R}^3$

$$\boldsymbol{\xi}(\psi, s, t) = (R(\psi, s, t) \cos(\psi), R(\psi, s, t) \sin(\psi), s). \quad (3)$$

Then, the outer normal vector \mathbf{n} and the surface speed w are expressed by

$$\begin{aligned} \mathbf{n}(\boldsymbol{\xi}, t) &= \frac{\partial_\psi \boldsymbol{\xi} \times \partial_s \boldsymbol{\xi}}{\|\partial_\psi \boldsymbol{\xi} \times \partial_s \boldsymbol{\xi}\|} = \frac{\partial_\psi (R \sin(\psi)) \mathbf{e}_1 - \partial_\psi (R \cos(\psi)) \mathbf{e}_2 - R \partial_s R \mathbf{e}_3}{\sqrt{R^2 + (\partial_\psi R)^2 + R^2 (\partial_s R)^2}} \\ w(\boldsymbol{\xi}, t) &= \partial_t \boldsymbol{\xi} \cdot \hat{\mathbf{n}}(\boldsymbol{\xi}, t) = \frac{R \partial_t R}{\sqrt{R^2 + (\partial_\psi R)^2 + R^2 (\partial_s R)^2}} \end{aligned}$$

Since $\boldsymbol{\rho}(\psi, s, t) = \check{\mathbf{r}}(\boldsymbol{\xi}(\psi, s, t), t) = \boldsymbol{\gamma}(s, t) + \epsilon(R(\psi, s, t) \cos(\psi) \boldsymbol{\eta}_1(s, t) + R(\psi, s, t) \sin(\psi) \boldsymbol{\eta}_2(s, t))$ is a parameterization of $\Gamma_{lat}^*(t)$ in spatial points for fixed time t , the mean curvature H can be computed as

$$H = -\frac{1}{2} \frac{(\mathbf{n}^* \cdot \partial_{\psi\psi} \boldsymbol{\rho})(\partial_s \boldsymbol{\rho} \cdot \partial_s \boldsymbol{\rho}) - 2(\mathbf{n}^* \cdot \partial_{\psi s} \boldsymbol{\rho})(\partial_\psi \boldsymbol{\rho} \cdot \partial_s \boldsymbol{\rho}) + (\mathbf{n}^* \cdot \partial_{ss} \boldsymbol{\rho})(\partial_\psi \boldsymbol{\rho} \cdot \partial_\psi \boldsymbol{\rho})}{(\partial_\psi \boldsymbol{\rho} \cdot \partial_\psi \boldsymbol{\rho})(\partial_s \boldsymbol{\rho} \cdot \partial_s \boldsymbol{\rho}) - (\partial_\psi \boldsymbol{\rho} \cdot \partial_s \boldsymbol{\rho})^2}$$

with outer normal $\mathbf{n}^*(\boldsymbol{\rho}, t) = (\partial_\psi \boldsymbol{\rho} \times \partial_s \boldsymbol{\rho}) / \|\partial_\psi \boldsymbol{\rho} \times \partial_s \boldsymbol{\rho}\|$, see [10]. Hence, we have

$$\begin{aligned} H &= -\frac{1}{2 \left((1 - \epsilon h)^2 (R^2 + (\partial_\psi R)^2) + \epsilon^2 R^2 (\partial_s R)^2 \right)^{3/2}} \\ &\quad \left(\epsilon^{-1} (1 - \epsilon h)^3 \left(-R^2 + R \partial_{\psi\psi} R - 2(\partial_\psi R)^2 \right) \right. \\ &\quad + (1 - \epsilon h)^2 \left(((\partial_\psi R)^3 + R^2 \partial_\psi R) (\sin(\psi) \partial_1 h - \cos(\psi) \partial_2 h) + (R^2 + (\partial_\psi R)^2) h \right) \\ &\quad + \epsilon (1 - \epsilon h) \left(R \partial_{\psi\psi} R (\partial_s R)^2 + R \partial_{ss} R (\partial_\psi R)^2 - 2R \partial_{\psi s} R \partial_\psi R \partial_s R - R^2 (\partial_s R)^2 + R^3 \partial_{ss} R \right) \\ &\quad + \epsilon^2 R \partial_s R \left((2R \partial_\psi R \partial_s R \sin(\psi) - (\partial_\psi R)^2 \partial_s R \cos(\psi)) \partial_1 h \right. \\ &\quad \left. + (-2R \partial_\psi R \partial_s R \cos(\psi) - (\partial_\psi R)^2 \partial_s R \sin(\psi)) \partial_2 h + R \partial_s R h + (R^2 + (\partial_\psi R)^2) \partial_s h \right) \Big). \end{aligned}$$

The kinematic and dynamic boundary conditions are formulated as

$$(\mathbf{u}(\boldsymbol{\xi}, t) - \partial_t \boldsymbol{\xi}) \cdot (\partial_\psi \boldsymbol{\xi} \times \partial_s \boldsymbol{\xi}) = 0, \quad (\mathbf{S} + \frac{\epsilon}{\text{We}} JH\mathbf{G})(\boldsymbol{\xi}, t) \cdot (\partial_\psi \boldsymbol{\xi} \times \partial_s \boldsymbol{\xi}) = \mathbf{0}.$$

Considering the bottom boundary $\Gamma_{bot}(t) = \mathcal{A}(L(t), t) \times \{L(t)\}$, we have to distinguish two scenarios. If $|\mathcal{A}(L(t), t)| = 0$, no further boundary conditions are necessary since the lateral surface equals the free surface up to a null set. On the other hand, if $|\mathcal{A}(L(t), t)| \neq 0$ holds, the bottom surface is planar in the coordinates and has the outer normal vector \mathbf{e}_3 in accordance to Ass 4. Due to the linearity of the coordinate transformation in (x_1, x_2) , the bottom surface in the spatial geometry inherits the planar shape and shows thus no mean curvature, i.e. $H = 0$. This leads to the following kinematic and dynamic boundary conditions of $\Gamma_{bot}(t)$

$$\frac{dL(t)}{dt} = u_3(\mathbf{x}, t), \quad (\mathbf{S} \cdot \mathbf{e}_3)(\mathbf{x}, t) = \mathbf{0}.$$

The initial condition $L(0) = 0$ that is generally equivalent to $\Omega(0) = \emptyset$ of the free BVP closes additionally the derived ordinary differential equation for the length in the second scenario.

Proceeding with the study of the inflow conditions, the inflow boundary Γ_{in}^* is considered to be planar with center point γ_0 and inner normal $\boldsymbol{\tau}_0$. In correspondence to Ass 4,

$$\gamma(0, t) = \gamma_0, \quad \partial_s \gamma(0, t) = \boldsymbol{\tau}_0 \quad (4)$$

hold. In addition, the relations for inflow velocity profile and slenderness parameter Eqs (1),(2) can be reformulated as

$$|\Gamma_{in}| = |\mathcal{A}|(0, t) = 1 \quad (5)$$

$$\int_{\Gamma_{in}} \mathbf{v}_{in} \cdot \boldsymbol{\tau}_0 \, d\mathcal{A} = \int_{\mathcal{A}(0,t)} \mathbf{v}_{in} \cdot \boldsymbol{\tau}_0 \, dx_1 dx_2 = 1. \quad (6)$$

Due to the coordinate transformation, the original boundary conditions (cf. Eqs (1),(2)) become independent of ϵ in the scaled curvilinear coordinates. This ϵ -independence of Eqs (5),(6) is utilized in the definition of the fiber family for the coming asymptotic analysis. The free BVP is embedded for a fixed slenderness parameter $\epsilon = \epsilon_0$ in a family of self-similar problems corresponding to parameters $\epsilon \leq \epsilon_0$ that are characterized by a fixed inflow domain in scaled curvilinear coordinates $(\Gamma_{in})_\epsilon = \Gamma_{in}$ as well as a fixed inflow velocity $(\mathbf{v}_{in})_\epsilon = \mathbf{v}_{in}$.

Summarizing the full set of equations for the fiber family, the variables depending on the slenderness parameter are marked with subscript ϵ . The unknowns are the field variables \mathbf{v}_ϵ , \mathbf{u}_ϵ , p_ϵ and the geometry variables L_ϵ , γ_ϵ , R_ϵ . All other occurring quantities are defined by the geometry.

Balance laws, $\mathbf{x} \in \Omega_\epsilon(t)$

$$\begin{aligned} \partial_t J_\epsilon(\mathbf{x}, t) + \nabla_{\mathbf{x}} \cdot (J_\epsilon \mathbf{u}_\epsilon)(\mathbf{x}, t) &= 0 \\ \partial_t (J_\epsilon \mathbf{v}_\epsilon)(\mathbf{x}, t) + \nabla_{\mathbf{x}} \cdot (\mathbf{u}_\epsilon \otimes J_\epsilon \mathbf{v}_\epsilon)(\mathbf{x}, t) &= \nabla_{\mathbf{x}} \cdot \mathbf{S}_\epsilon^T(\mathbf{x}, t) + (J_\epsilon \mathbf{f}_\epsilon)(\mathbf{x}, t) \end{aligned}$$

Coupling condition

$$\mathbf{u}_\epsilon = (\mathbf{v}_\epsilon - \mathbf{q}_\epsilon) \cdot \mathbf{G}_\epsilon$$

Lateral surface conditions, $\boldsymbol{\xi}_\epsilon \in (\Gamma_{lat})_\epsilon(t)$

$$(\mathbf{u}_\epsilon(\boldsymbol{\xi}_\epsilon, t) - \partial_t \boldsymbol{\xi}_\epsilon) \cdot (\partial_\psi \boldsymbol{\xi}_\epsilon \times \partial_s \boldsymbol{\xi}_\epsilon) = 0, \quad (\mathbf{S}_\epsilon + \frac{\epsilon}{\text{We}} J_\epsilon H_\epsilon \mathbf{G}_\epsilon)(\boldsymbol{\xi}_\epsilon, t) \cdot (\partial_\psi \boldsymbol{\xi}_\epsilon \times \partial_s \boldsymbol{\xi}_\epsilon) = \mathbf{0}$$

and if $|(\Gamma_{bot})_\epsilon(t)| > 0$: Bottom surface conditions, $\mathbf{x} \in (\Gamma_{bot})_\epsilon(t)$

$$\frac{dL_\epsilon(t)}{dt} = u_{3,\epsilon}(\mathbf{x}, t), \quad (\mathbf{S}_\epsilon \cdot \mathbf{e}_3)(\mathbf{x}, t) = \mathbf{0}$$

Inflow boundary condition, $\mathbf{x} \in (\Gamma_{in})_\epsilon$ $\mathbf{v}_\epsilon(\mathbf{x}, t) = \mathbf{v}_{in}(\mathbf{x})$

Geometry conditions

$$\|\partial_s \gamma_\epsilon\| = 1, \quad \gamma_\epsilon(0, t) = \gamma_0, \quad \partial_s \gamma_\epsilon(0, t) = \tau_0, \quad \int_{\mathcal{A}_\epsilon(s,t)} x_1 dx_1 dx_2 = \int_{\mathcal{A}_\epsilon(s,t)} x_2 dx_1 dx_2 = 0$$

Initial condition

$$L_\epsilon(0) = 0$$

3 Asymptotic Analysis

The derivation of the one-dimensional asymptotic fiber model from the three-dimensional free BVP is based on the cross-sectional averaging of the balance laws. Thereby, the asymptotic expansions in zeroth and first order yield the necessary cross-sectional profile properties of the unknowns. The corresponding boundary conditions are deduced from the comparison of the volume averaged one- and three-dimensional balance laws.

3.1 Cross-sectional Averaging

For the formulation of the cross-sectional averaged balance laws special integration rules are provided. Therefore, the following conventions are introduced

$$\langle f \rangle_{\mathcal{A}(s,t)} = \int_{\mathcal{A}(s,t)} f(x_1, x_2, s, t) dx_1 dx_2, \quad \langle f \rangle_{\partial \mathcal{A}(s,t)} = \int_{\partial \mathcal{A}(s,t)} \frac{f}{\sqrt{n_1^2 + n_2^2}} dl,$$

where f denotes a differentiable and integrable scalar-, vector- or tensor-valued function on $\Omega(t)$, \mathcal{A} a cross-section and \mathbf{n} the unit outer normal vector on the lateral surface $\Gamma_{lat}(t)$.

Lemma 5 *Let f be a differentiable and integrable scalar-, vector- or tensor-valued function on $\Omega(t)$, then the following computation rules are valid*

$$\langle \partial_s f \rangle_{\mathcal{A}(s,t)} = \partial_s \langle f \rangle_{\mathcal{A}(s,t)} + \langle f n_3 \rangle_{\partial \mathcal{A}(s,t)}, \quad \langle \partial_t f \rangle_{\mathcal{A}(s,t)} = \partial_t \langle f \rangle_{\mathcal{A}(s,t)} - \langle f w \rangle_{\partial \mathcal{A}(s,t)}.$$

Lemma 5 can be concluded from the Reynolds-Transport Theorem, [8]. The stated integration rules can be extended on arbitrary vector \mathbf{m} and tensor \mathbf{M} fields possessing the same properties as f by help of the Gauss Theorem

$$\langle \nabla \cdot \mathbf{m} \rangle_{\mathcal{A}(s,t)} = \partial_s \langle \mathbf{m} \cdot \mathbf{e}_3 \rangle_{\mathcal{A}(s,t)} + \langle \mathbf{m} \cdot \mathbf{n} \rangle_{\partial \mathcal{A}(s,t)}, \quad \langle \nabla \cdot \mathbf{M}^T \rangle_{\mathcal{A}(s,t)} = \partial_s \langle \mathbf{M} \cdot \mathbf{e}_3 \rangle_{\mathcal{A}(s,t)} + \langle \mathbf{M} \cdot \mathbf{n} \rangle_{\partial \mathcal{A}(s,t)}$$

Applying them on the three-dimensional balance laws of our family problem and incorporating the lateral surface conditions give one-dimensional balance laws that will play the crucial role for the closing of the asymptotic expansions in the following subsections.

Theorem 6 (Cross-sectional Averaged Balance Laws) *Let a solution of the fiber family BVP exist. Then the following cross-sectional integral relations hold*

$$\begin{aligned} \partial_t \langle J_\epsilon \rangle_{\mathcal{A}_\epsilon(s,t)} + \partial_s \langle J_\epsilon u_{3,\epsilon} \rangle_{\mathcal{A}_\epsilon(s,t)} &= 0 \\ \partial_t \langle J_\epsilon \mathbf{v}_\epsilon \rangle_{\mathcal{A}_\epsilon(s,t)} + \partial_s \langle J_\epsilon u_{3,\epsilon} \mathbf{v}_\epsilon \rangle_{\mathcal{A}_\epsilon(s,t)} &= \partial_s \langle \mathbf{S}_\epsilon \cdot \mathbf{e}_3 \rangle_{\mathcal{A}_\epsilon(s,t)} - \frac{\epsilon}{\text{We}} \langle J_\epsilon H_\epsilon \mathbf{G}_\epsilon \cdot \mathbf{n}_\epsilon \rangle_{\partial \mathcal{A}_\epsilon(s,t)} + \langle J_\epsilon \mathbf{f}_\epsilon \rangle_{\mathcal{A}_\epsilon(s,t)}. \end{aligned}$$

Using the parameterization ξ of $\Gamma_{lat}(t)$ in Eq (3), we can write the line integral explicitly as

$$\langle J_\epsilon H_\epsilon \mathbf{G}_\epsilon \cdot \mathbf{n}_\epsilon \rangle_{\partial \mathcal{A}_\epsilon(s,t)} = \int_0^{2\pi} \left(\epsilon(1 - \epsilon h_\epsilon) (\partial_\psi (R_\epsilon \sin(\psi)) \boldsymbol{\eta}_{1,\epsilon} - \partial_\psi (R_\epsilon \cos(\psi)) \boldsymbol{\eta}_{2,\epsilon}) - \epsilon^2 R_\epsilon \partial_s R_\epsilon \boldsymbol{\tau}_\epsilon \right) H_\epsilon d\psi.$$

3.2 Asymptotic Expansions

The fact that the fiber domain itself depends on ϵ challenges the asymptotic expansion of the free BVP equations. This difficulty is handled by extending all field quantities on the domain $\cup_{\epsilon < \epsilon_0} \Omega_\epsilon(t)$ and presupposing that their restrictions on $\Omega_\epsilon(t)$ are solutions of the respective ϵ -problem.

For the underlying geometry variables, regular power series expansions in ϵ are set up

$$\begin{aligned} L_\epsilon(t) &= L^{(0)}(t) + \epsilon L^{(1)}(t) + \mathcal{O}(\epsilon^2) \\ \gamma_\epsilon(s, t) &= \gamma^{(0)}(s, t) + \epsilon \gamma^{(1)}(s, t) + \mathcal{O}(\epsilon^2) \\ R_\epsilon(\psi, s, t) &= R^{(0)}(\psi, s, t) + \epsilon R^{(1)}(\psi, s, t) + \mathcal{O}(\epsilon^2) \end{aligned}$$

with $s \in [0, \max_{\epsilon < \epsilon_0} L_\epsilon(t))$ and $\psi \in [0, 2\pi)$. The field variables \mathbf{v}_ϵ and p_ϵ are analogously expanded

$$\begin{aligned} \mathbf{v}_\epsilon(\mathbf{x}, t) &= \mathbf{v}^{(0)}(\mathbf{x}, t) + \epsilon \mathbf{v}^{(1)}(\mathbf{x}, t) + \mathcal{O}(\epsilon^2) \\ p_\epsilon(\mathbf{x}, t) &= p^{(0)}(\mathbf{x}, t) + \epsilon p^{(1)}(\mathbf{x}, t) + \mathcal{O}(\epsilon^2) \end{aligned}$$

for $\mathbf{x} \in \cup_{\epsilon < \epsilon_0} \Omega_\epsilon(t)$. Then, the coupling condition determines the expansion of \mathbf{u} whose leading order term is $\mathcal{O}(\epsilon^{-1})$ due to the decomposition of $\mathbf{G}_\epsilon = \mathbf{g}_{i,\epsilon} \otimes \mathbf{e}_i$

$$\mathbf{u}_\epsilon(\mathbf{x}, t) = \epsilon^{-1} \mathbf{u}^{(-1)}(\mathbf{x}, t) + \mathbf{u}^{(0)}(\mathbf{x}, t) + \epsilon \mathbf{u}^{(1)}(\mathbf{x}, t) + \mathcal{O}(\epsilon^2).$$

Since particularly $\mathbf{g}_{3,\epsilon} \sim \mathcal{O}(1)$, $u_3^{(-1)} = 0$ holds. The body force densities are assumed to be $\mathbf{f}^{(0)}(s)$ in leading order which stands in accordance to the gravitational and rotational forces being considered in the application. Concerning the mean curvature H_ϵ , the expansion reads $H_\epsilon = \epsilon^{-1} H^{(-1)} + H^{(0)} + \mathcal{O}(\epsilon)$ where the dominant terms are

$$\begin{aligned} H^{(-1)} &= \frac{1}{2} \frac{(R^{(0)})^2 - R^{(0)} \partial_{\psi\psi} R^{(0)} + 2(\partial_\psi R^{(0)})^2}{((R^{(0)})^2 + (\partial_\psi R^{(0)})^2)^{3/2}} \\ H^{(0)} &= \frac{1}{2} \frac{1}{((R^{(0)})^2 + (\partial_\psi R^{(0)})^2)^{3/2}} \\ &\quad \left((-R^{(0)})^2 - (\partial_\psi R^{(0)})^2 h^{(0)} + ((\partial_\psi R^{(0)})^3 + (R^{(0)})^2 \partial_\psi R^{(0)}) (\cos(\psi) \partial_2 h^{(0)} - \sin(\psi) \partial_1 h^{(0)}) \right. \\ &\quad \left. + 2R^{(0)} R^{(1)} - R^{(0)} \partial_{\psi\psi} R^{(1)} - R^{(1)} \partial_{\psi\psi} R^{(0)} + 4\partial_\psi R^{(0)} \partial_\psi R^{(1)} \right. \\ &\quad \left. - 3 \frac{R^{(0)} R^{(1)} + \partial_\psi R^{(0)} \partial_\psi R^{(1)}}{(R^{(0)})^2 + (\partial_\psi R^{(0)})^2} ((R^{(0)})^2 - R^{(0)} \partial_{\psi\psi} R^{(0)} + 2(\partial_\psi R^{(0)})^2) \right) \end{aligned}$$

Thereby, $2H^{(-1)}$ represents the curvature in zeroth order of the boundary curve in polar coordinates. Note that we impose no restrictions on γ_ϵ in comparison to Decent and Wallwork [5, 6, 34] who assume a stationary center-line in leading order.

It makes no sense to study the asymptotics of the sets $\Omega_\epsilon(t)$, $(\Gamma_{lat})_\epsilon(t)$, $(\Gamma_{bot})_\epsilon(t)$ and $\mathcal{A}_\epsilon(s, t)$ in analogon to the functions. However, the limit case $\epsilon \rightarrow 0$ exists and this reference geometry is denoted by $\Omega_0(t)$, $(\Gamma_{lat})_0(t)$, $(\Gamma_{bot})_0(t)$ and $\mathcal{A}_0(s, t)$. The reference geometry is expected to satisfy $|(\Gamma_{bot})_0(t)| > 0$ – even in cases where $|(\Gamma_{bot})_\epsilon(t)| = 0$ holds –, because the scaled bottom surface becomes planar for $\epsilon \rightarrow 0$. This stands in no contradiction to our asymptotic expansion of the geometrical quantities, since we always consider open intervals for the fiber ending. As we see, the asymptotically derived one-dimensional fiber model allows finite bottom surfaces.

Corresponding to the reference geometry, the normal vectors and the surface speed in parametric version are given by $\mathbf{n}_0(\boldsymbol{\xi}^{(0)}, t) = (\partial_\psi \boldsymbol{\xi}^{(0)} \times \partial_s \boldsymbol{\xi}^{(0)}) / \|\partial_\psi \boldsymbol{\xi}^{(0)} \times \partial_s \boldsymbol{\xi}^{(0)}\|$ and $w_0(\boldsymbol{\xi}^{(0)}, t) = \partial_t \boldsymbol{\xi}^{(0)}$.

$\mathbf{n}_0(\boldsymbol{\xi}^{(0)}, t)$. Then, the lateral surface conditions read

$$\begin{aligned} 0 = & \mathbf{u}^{(-1)}(\boldsymbol{\xi}^{(0)}, t) \cdot (\partial_\psi \boldsymbol{\xi}^{(0)} \times \partial_s \boldsymbol{\xi}^{(0)}) \\ & + \epsilon \left((\mathbf{u}^{(0)}(\boldsymbol{\xi}^{(0)}, t) + \boldsymbol{\xi}^{(1)} \cdot \nabla \mathbf{u}^{(-1)}(\boldsymbol{\xi}^{(0)}, t) - \partial_t \boldsymbol{\xi}^{(0)}) \cdot (\partial_\psi \boldsymbol{\xi}^{(0)} \times \partial_s \boldsymbol{\xi}^{(0)}) \right. \\ & \left. + \mathbf{u}^{(-1)}(\boldsymbol{\xi}^{(0)}, t) \cdot (\partial_\psi \boldsymbol{\xi}^{(0)} \times \partial_s \boldsymbol{\xi}^{(1)} + \partial_\psi \boldsymbol{\xi}^{(1)} \times \partial_s \boldsymbol{\xi}^{(0)}) \right) + \mathcal{O}(\epsilon^2) \end{aligned} \quad (7)$$

and

$$\begin{aligned} \mathbf{0} = & \mathbf{S}^{(0)}(\boldsymbol{\xi}^{(0)}, t) \cdot (\partial_\psi \boldsymbol{\xi}^{(0)} \times \partial_s \boldsymbol{\xi}^{(0)}) \\ & + \epsilon \left(((\mathbf{S}^{(1)}(\boldsymbol{\xi}^{(0)}, t) + \frac{1}{\text{We}} H^{(-1)} \mathbf{G}^{(-1)}(\boldsymbol{\xi}^{(0)}, t)) + \boldsymbol{\xi}^{(1)} \cdot \nabla \mathbf{S}^{(0)}(\boldsymbol{\xi}^{(0)}, t)) \cdot (\partial_\psi \boldsymbol{\xi}^{(0)} \times \partial_s \boldsymbol{\xi}^{(0)}) \right. \\ & \left. + \mathbf{S}^{(0)}(\boldsymbol{\xi}^{(0)}, t) \cdot (\partial_\psi \boldsymbol{\xi}^{(0)} \times \partial_s \boldsymbol{\xi}^{(1)} + \partial_\psi \boldsymbol{\xi}^{(1)} \times \partial_s \boldsymbol{\xi}^{(0)}) \right) + \mathcal{O}(\epsilon^2). \end{aligned} \quad (8)$$

by using Taylor expansion around the reference geometry. Since Eqs (7),(8) lead to boundary conditions in zeroth and first order for the reference geometry, the unknowns defined on $\cup_{\epsilon < \epsilon_0} \Omega_\epsilon(t)$ are assumed to satisfy the balance laws on $\Omega_0(t)$.

3.3 Balance Laws for Radial Cross-sections

The application of Th 6 requires knowledge about the relation between the fiber cross-sections and their boundary curves. The evolution of the cross-sectional shape for nearly straight fibers is governed by a quasi two-dimensional free boundary problem similar to two-dimensional Stokes flow with a surface tension driven boundary and described by conformal mappings in Cummings et.al. [4]. Since the shape tends to a circle under surface tension, we restrict our general considerations on the intuitive case of a circular nozzle and consequently of radial cross-sections, i.e. $R^{(0)} = R^{(0)}(s, t)$, $R^{(1)} = R^{(1)}(s, t)$, which stands in accordance to our center-line condition. Then, the mean curvature reduces to

$$H^{(-1)} = \frac{1}{2R^{(0)}}, \quad H^{(0)} = \frac{-R^{(0)}h^{(0)} - R^{(1)}}{2(R^{(0)})^2} \quad (9)$$

Focusing on the family of balance laws with lateral surface conditions (lateral problem) in Sec 2.3, we derive zeroth and first order equations in ϵ with closure conditions that result in the desired one-dimensional asymptotic fiber model on the radial reference geometry. Since the form of the zeroth and first order equations is similar, a general solution theory oriented on [8] is pre-stated.

Lemma 7 *Let $\mathcal{D} \subset \mathbb{R}^2$ be a bounded domain with outer normal vector \mathbf{n} on $\partial\mathcal{D}$. Let $\mathbf{T}(\mathbf{x}) \in \mathbb{R}^{2 \times 2}$ be a regular symmetric matrix for $\mathbf{x} \in \mathcal{D}$. Then, $\mathbf{T} = \mathbf{0}$ is the unique solution of the following boundary value problem*

$$\begin{aligned} \nabla \cdot \mathbf{T}^T &= \mathbf{0}, \quad \Delta \text{tr} \mathbf{T} = 0 \quad \text{in } \mathcal{D} \\ \mathbf{T} \cdot \mathbf{n} &= \mathbf{0} \quad \text{on } \partial\mathcal{D} \end{aligned}$$

Proof: Obviously, $\mathbf{T} = \mathbf{0}$ is a solution. Thus, the uniqueness remains to be shown. The symmetry and the zero divergence implies the existence of the Airy-stress function $\alpha : \mathcal{D} \rightarrow \mathbb{R}$ with

$$\mathbf{T} = \begin{pmatrix} \partial_{22}\alpha & -\partial_{12}\alpha \\ -\partial_{12}\alpha & \partial_{11}\alpha \end{pmatrix}.$$

Consequently, $\text{tr}\mathbf{T} = \Delta\alpha$. This results in the biharmonic problem $\Delta\Delta\alpha = 0$ whose boundary condition $\nabla\alpha = (c_1, c_2) = \text{const}$ can be concluded from $\mathbf{T} \cdot \mathbf{n} = \mathbf{0}$ on $\partial\mathcal{D}$. Its general solution reads $\alpha = c_1x_1 + c_2x_2 + c_3$ with constant c_3 . Hence, $\mathbf{T} = \mathbf{0}$. \square

Theorem 8 *Let $\mathcal{D} \subset \mathbb{R}^2$ be a bounded domain with outer normal vector \mathbf{n} on $\partial\mathcal{D}$ and let $c \in \mathbb{R}$ be constant. Let $f : \mathcal{D} \rightarrow \mathbb{R}$, $\Phi : \mathcal{D} \rightarrow \mathbb{R}^2$ and $\varphi : \mathcal{D} \rightarrow \mathbb{R}$ be sufficiently smooth.*

1. *The solution of the boundary value problem*

$$\begin{aligned} \nabla \cdot \Phi &= c, & \nabla(\nabla \cdot \Phi) + \Delta\Phi &= \nabla f & \text{in } \mathcal{D} \\ (\nabla\Phi + \nabla\Phi^T) \cdot \mathbf{n} &= f\mathbf{n} & & & \text{on } \partial\mathcal{D} \end{aligned}$$

has the following form with constant parameters a , b_1 and b_2

$$\Phi_1(x_1, x_2) = \frac{c}{2}x_1 - ax_2 + b_1, \quad \Phi_2(x_1, x_2) = \frac{c}{2}x_2 + ax_1 + b_2, \quad f = c.$$

2. *The solution of the boundary value problem*

$$\Delta\varphi = 0 \quad \text{in } \mathcal{D}, \quad \nabla\varphi \cdot \mathbf{n} = 0 \quad \text{on } \partial\mathcal{D}$$

is constant, i.e. $\varphi(x_1, x_2) = c$.

Proof: For the two-dimensional stress-free Stokes equations, the matrix-valued function

$$\mathbf{T} = \begin{pmatrix} 2\partial_1\Phi_1 - f & \partial_1\Phi_2 + \partial_2\Phi_1 \\ \partial_1\Phi_2 + \partial_2\Phi_1 & 2\partial_2\Phi_2 - f \end{pmatrix}$$

satisfies the boundary value problem of Lem 7. Thus, $\mathbf{T} = \mathbf{0}$ which implies $\partial_1\Phi_1 = \partial_2\Phi_2 = f/2$ and $\partial_1\Phi_2 + \partial_2\Phi_1 = 0$. Applying $\nabla \cdot \Phi = c$ results in $f = c$ which leads to the stated solution. For the Laplace equation with Neumann condition the solution form is trivial. \square

Zeroth Order

Using the zeroth order stress tensor

$$\mathbf{S}^{(0)} = \frac{1}{\text{Re}} \left((\partial_\alpha u_\beta^{(-1)} + \partial_\beta u_\alpha^{(-1)}) (\boldsymbol{\eta}_\alpha^{(0)} \otimes \mathbf{e}_\beta) + (\partial_\alpha u_3^{(0)}) (\boldsymbol{\tau}^{(0)} \otimes \mathbf{e}_\alpha) \right)$$

and Eqs (7),(8), the balance laws with lateral surface conditions on the reference geometry read

$$\begin{aligned} \partial_\alpha u_\alpha^{(-1)} &= 0, & (\partial_{\alpha\beta} u_\beta^{(-1)} + \partial_{\beta\alpha} u_\alpha^{(-1)}) \boldsymbol{\eta}_\alpha^{(0)} + (\partial_{\alpha\alpha} u_3^{(0)}) \boldsymbol{\tau}^{(0)} &= \mathbf{0} & \text{in } \Omega_0(t) \\ (\partial_\alpha u_\beta^{(-1)} + \partial_\beta u_\alpha^{(-1)}) n_{0,\beta} \boldsymbol{\eta}_\alpha^{(0)} + \partial_\alpha u_3^{(0)} n_{0,\alpha} \boldsymbol{\tau}^{(0)} &= \mathbf{0} & & & \text{on } (\Gamma_{lat})_0(t) \end{aligned}$$

Lemma 9 (Cross-sectional Profile Properties in Zeroth Order) *Let the kinematic boundary condition fulfill $\mathbf{u}^{(-1)} \cdot \mathbf{n}_0 = 0$. Then, the solution of the stated zeroth order lateral problem satisfies*

$$\begin{aligned} u_1^{(-1)} &= -a(s, t)x_2, & u_3^{(0)} &= u_3^{(0)}(s, t), \\ u_2^{(-1)} &= a(s, t)x_1 \end{aligned}$$

Proof: Applying Th 8.1 for $u_1^{(-1)}$ and $u_2^{(-1)}$ yields

$$u_1^{(-1)} = -a(s, t)x_2 + b_1(s, t), \quad u_2^{(-1)} = a(s, t)x_1 + b_2(s, t).$$

Note that $f = c = 0$ are consistently given. The satisfaction of the kinematic boundary condition requires the vanishing of the constants $b_1(s, t)$ and $b_2(s, t)$, i.e. $b_1 = b_2 = 0$, but it is independent of the choice of $a(s, t)$ in case of the considered circular cross-sections. The result for $u_3^{(0)}$ follows directly from Th 8.2. \square

As consequence of the lemma the zeroth order velocity and stress satisfy

$$\mathbf{v}^{(0)} = u_\alpha^{(-1)} \boldsymbol{\eta}_\alpha^{(0)} + u_3^{(0)} \boldsymbol{\tau}^{(0)} + \partial_t \boldsymbol{\gamma}^{(0)}, \quad \mathbf{S}^{(0)} = \mathbf{0}.$$

Note that for non-circular cross-sections $b_1 = b_2 = 0$ also hold by the additional help of the center-line condition. Moreover, $a(s, t)$ must vanish to fulfill the kinematic boundary condition. Since any slight perturbations at the nozzle destroy the circular cross-sectional profile, $a = 0$ and thus $\mathbf{u}^{(-1)} = \mathbf{0}$ are the only relevant solutions. The degree of freedom in the circular case is gained from the coordinate transformation. However, the appearing singularity has no effect on our final result due to the imposed center-line condition as we will see in the following.

First Order

With the results of zeroth order and the deduced first order stress tensor

$$\mathbf{S}^{(1)} = -p^{(0)} (\boldsymbol{\eta}_\alpha^{(0)} \otimes \mathbf{e}_\alpha) + \frac{1}{\text{Re}} \left((\partial_\alpha u_\beta^{(0)} + \partial_\beta u_\alpha^{(0)}) (\boldsymbol{\eta}_\alpha^{(0)} \otimes \mathbf{e}_\beta) + (\partial_\alpha u_3^{(1)} + \partial_s u_\alpha^{(-1)}) (\boldsymbol{\tau}^{(0)} \otimes \mathbf{e}_\alpha) \right),$$

the first order lateral problem reads

$$\begin{aligned} \partial_\alpha u_\alpha^{(0)} + \partial_s u_3^{(0)} &= 0, & \left(\partial_{\alpha\beta} u_\beta^{(0)} + \partial_{\beta\alpha} u_\alpha^{(0)} - \text{Re} \partial_\alpha p^{(0)} \right) \boldsymbol{\eta}_\alpha^{(0)} + \partial_{\alpha\alpha} u_3^{(1)} \boldsymbol{\tau}^{(0)} &= \mathbf{0} \quad \text{in } \Omega_0(t) \\ \left((\partial_\alpha u_\beta^{(0)} + \partial_\beta u_\alpha^{(0)}) n_{0,\beta} + \text{Re}(-p^{(0)} + \frac{1}{\text{We}} H^{(-1)}) n_{0,\alpha} \right) \boldsymbol{\eta}_\alpha^{(0)} + \partial_\alpha u_3^{(1)} n_{0,\alpha} \boldsymbol{\tau}^{(0)} &= \mathbf{0} \quad \text{on } (\Gamma_{lat})_0(t) \end{aligned}$$

The validity of the boundary conditions on the radial reference geometry is concluded from Eqs (7),(8) using $\mathbf{u}^{(-1)} = a(s, t)(-x_2 \mathbf{e}_1 + x_1 \mathbf{e}_2)$ and $\mathbf{S}^{(0)} = \mathbf{0}$.

Lemma 10 (Cross-sectional Profile Properties in First Order) *Let the kinematic boundary condition fulfill $\mathbf{u}^{(0)} \cdot \mathbf{n}_0 = w_0$. Then, the solution of the first order lateral problem satisfies*

$$\begin{aligned} u_1^{(0)} &= -\frac{1}{2} \partial_s u_3^{(0)}(s, t)x_1 - d(s, t)x_2 & p^{(0)} &= -\frac{1}{\text{Re}} \partial_s u_3^{(0)}(s, t) + \frac{1}{\text{We}} H^{(-1)} \\ u_2^{(0)} &= -\frac{1}{2} \partial_s u_3^{(0)}(s, t)x_2 + d(s, t)x_1 & u_3^{(1)} &= u_3^{(1)}(s, t). \end{aligned}$$

with $H^{(-1)} = 1/(2R^{(0)})$.

Proof: Since $H^{(-1)}$ is constant for circular cross-sections, Th 8 can be applied. The strategy of proof is analogous to the one for the zeroth order problem. \square

Apart from the vanishing of the additive constants in the proof of $u_1^{(0)}$ and $u_2^{(0)}$, the satisfaction of the kinematic boundary condition in Lem 10 leads also to the – cross-sectional averaged – continuity equation for the asymptotic fiber model stated in Eq (10). This result is not so surprising since we impose a restriction on the shape of the boundary by presupposing the cross-sections to be circular. It just confirms the consistency of our assumption and the asymptotic analysis. The determination of the twist parameter $d(s, t)$, cf. [7], is not necessary, since it decouples from our final model.

Closure

Considering the cross-sectional averaged balance laws of Th 6, only the axial effect of the second order stress tensor is of interest, since consistently $\mathbf{S}^{(0)} \cdot \mathbf{e}_3 = \mathbf{S}^{(1)} \cdot \mathbf{e}_3 = \mathbf{0}$. Using the results of zeroth and first order it particularly reads

$$\mathbf{S}^{(2)} \cdot \mathbf{e}_3 = -p^{(0)} \boldsymbol{\tau}^{(0)} + \frac{1}{\text{Re}} \left(2(\partial_s u_3^{(0)} - u_\alpha^{(-1)} \partial_\alpha h) \boldsymbol{\tau}^{(0)} + \partial_s u_\alpha^{(-1)} \boldsymbol{\eta}_\alpha^{(0)} \right)$$

and hence

$$\langle \mathbf{S}^{(2)} \cdot \mathbf{e}_3 \rangle_{\mathcal{A}_0} = \left(-p^{(0)} + \frac{2}{\text{Re}} \partial_s u_3^{(0)} \right) \boldsymbol{\tau}^{(0)} |\mathcal{A}_0| = \left(\frac{3}{\text{Re}} \partial_s u_3^{(0)} |\mathcal{A}_0| - \frac{\sqrt{\pi}}{2\text{We}} \sqrt{|\mathcal{A}_0|} \right) \boldsymbol{\tau}^{(0)}$$

by applying the center-line condition and the assumption of circular cross-sections. With Eq (9), the line integral over the boundary vanishes consistently in zeroth order. In first order it is explicitly given by

$$(\langle JH\mathbf{G} \cdot \mathbf{n} \rangle_{\partial \mathcal{A}_\epsilon})^{(1)} = -\pi \partial_s (R^{(0)} \boldsymbol{\tau}^{(0)}) = -\sqrt{\pi} \partial_s (\sqrt{|\mathcal{A}_0|} \boldsymbol{\tau}^{(0)})$$

Thus, the averaged balance laws in their leading order result in the following asymptotic fiber model

$$\partial_t |\mathcal{A}_0| + \partial_s (u_3^{(0)} |\mathcal{A}_0|) = 0 \tag{10}$$

$$\partial_t (\langle \mathbf{v}^{(0)} \rangle_{\mathcal{A}_0}) + \partial_s (u_3^{(0)} \langle \mathbf{v}^{(0)} \rangle_{\mathcal{A}_0}) = \partial_s \left(\left(\frac{3}{\text{Re}} \partial_s u_3^{(0)} |\mathcal{A}_0| + \frac{\sqrt{\pi}}{2\text{We}} \sqrt{|\mathcal{A}_0|} \right) \boldsymbol{\tau}^{(0)} \right) + \mathbf{f}^{(0)} |\mathcal{A}_0|. \tag{11}$$

with the respective coupling and geometry conditions

$$\begin{aligned} \langle \mathbf{v}^{(0)} \rangle_{\mathcal{A}_0} &= (u_3^{(0)}(s, t) \boldsymbol{\tau}^{(0)}(s, t) + \partial_t \boldsymbol{\gamma}^{(0)}(s, t)) |\mathcal{A}_0| \\ \|\partial_s \boldsymbol{\gamma}^{(0)}\| &= 1. \end{aligned}$$

Only the cross-sectional averaged velocity – not the exact profile – is of interest in the momentum equation. Its exclusive dependence on the tangential intrinsic velocity and the dynamics of the center-line is deduced from the center-line condition.

3.4 Initial and Boundary Conditions for Radial Cross-sections

Closing the one-dimensional fiber model, Eqs (10),(11), requires the derivation of appropriate initial and boundary conditions in leading order.

Since $\Omega(0) = \emptyset$ holds, $L^{(0)}(0) = 0$ describes the initial condition. The inflow boundary conditions are accordingly to Eqs (4),(5)

$$\boldsymbol{\gamma}^{(0)}(0, t) = \boldsymbol{\gamma}_0, \quad \partial_s \boldsymbol{\gamma}^{(0)}(0, t) = \boldsymbol{\tau}_0, \quad |\mathcal{A}_0|(0, t) = 1$$

and additionally

$$u_3^{(0)}(0, t) = 1$$

which results from $\langle \mathbf{v}_{in} \rangle_{\mathcal{A}_0(0,t)} = \langle \mathbf{v}^{(0)} \rangle_{\mathcal{A}_0(0,t)} = u_3^{(0)}(0, t) \boldsymbol{\tau}_0$ with Eq (6). The boundary conditions at the free fiber end are concluded from the comparison of the volume averaged one- and three-dimensional balance laws in leading order. After plugging in the boundary conditions the volume

averaged three-dimensional equations read

$$\begin{aligned} \frac{d}{dt} \int_0^{L_\epsilon(t)} \langle J_\epsilon \rangle_{\mathcal{A}_\epsilon(s,t)} ds - \langle J_\epsilon \mathbf{u}_\epsilon \cdot \mathbf{e}_3 \rangle_{\mathcal{A}_\epsilon(0,t)} &= 0 \\ \frac{d}{dt} \int_0^{L_\epsilon(t)} \langle J_\epsilon \mathbf{v}_\epsilon \rangle_{\mathcal{A}_\epsilon(s,t)} ds - \langle J_\epsilon \mathbf{v}_\epsilon \mathbf{u}_\epsilon \cdot \mathbf{e}_3 \rangle_{\mathcal{A}_\epsilon(0,t)} &= -\langle \mathbf{S}_\epsilon \cdot \mathbf{e}_3 \rangle_{\mathcal{A}_\epsilon(0,t)} \\ &\quad - \frac{\epsilon}{\text{We}} \int_0^{L_\epsilon(t)} \langle J_\epsilon H_\epsilon \mathbf{G}_\epsilon \cdot \mathbf{n}_\epsilon \rangle_{\partial \mathcal{A}_\epsilon(s,t)} ds + \int_0^{L_\epsilon(t)} \langle J_\epsilon \mathbf{f}_\epsilon \rangle_{\mathcal{A}_\epsilon(s,t)} ds. \end{aligned}$$

Thereby, the integral over the bottom surface is zero since either $|\mathcal{A}(L(t), t)| = 0$ or $H = 0$. Thus, the integral over the free fiber surface reduces to the integral over the lateral surface, and additionally $\int_{(\Gamma_{lat})_\epsilon(t)} f d\mathcal{A} = \int_0^{L_\epsilon(t)} \langle f \rangle_{\partial \mathcal{A}_\epsilon} ds$ holds for any integrable function f . Consequently, we obtain in leading order

$$\begin{aligned} \frac{dL^{(0)}(t)}{dt} |\mathcal{A}_0|(L^{(0)}(t), t) + \int_0^{L^{(0)}(t)} \partial_t |\mathcal{A}_0| ds - (u_3^{(0)} |\mathcal{A}_0|)(0, t) &= 0 \\ \frac{d}{dt} \int_0^{L^{(0)}(t)} \langle \mathbf{v}^{(0)} \rangle_{\mathcal{A}_0(s,t)} ds - u_3^{(0)}(0, t) \langle \mathbf{v}^{(0)} \rangle_{\mathcal{A}_0(0,t)} &= - \left(\left(\frac{3}{\text{Re}} \partial_s u_3^{(0)} |\mathcal{A}_0| - \frac{\sqrt{\pi}}{2\text{We}} \sqrt{|\mathcal{A}_0|} \boldsymbol{\tau}^{(0)} \right) (0, t) \right. \\ &\quad \left. + \frac{\sqrt{\pi}}{\text{We}} \sqrt{|\mathcal{A}_0|} \boldsymbol{\tau}^{(0)} \Big|_{s=0}^{L^{(0)}(t)} + \int_0^{L^{(0)}(t)} \mathbf{f}^{(0)} |\mathcal{A}_0| ds. \right) \end{aligned}$$

Integrating the one-dimensional fiber equations, Eqs (10),(11), over $L^{(0)}(t)$ leads to a similar set of equations. Their difference to the volume averaged three-dimensional balance laws are the desired kinematic and dynamic boundary conditions, i.e.

$$\frac{dL^{(0)}(t)}{dt} = u_3^{(0)}(L^{(0)}(t), t), \quad (|\mathcal{A}_0| \partial_s u_3^{(0)})(L^{(0)}(t), t) = \frac{\sqrt{\pi}}{6} \frac{\text{Re}}{\text{We}} \sqrt{|\mathcal{A}_0|}(L^{(0)}(t), t).$$

Setting $u = u_3^{(0)}$, $\mathbf{v} = \langle \mathbf{v}^{(0)} \rangle_{\mathcal{A}_0} / |\mathcal{A}_0|$, $A = |\mathcal{A}_0|$ and dropping the superscript at the variables and the body forces of leading order, we obtain the one-dimensional model equations stated in Sec 1.

4 Numerical Results and Discussion

The asymptotic one-dimensional model describes the spinning of a slender curved inertial viscous Newtonian fiber with surface tension. It determines the dynamics of the fiber center-line $\boldsymbol{\gamma}$, the cross-sectional area A , the intrinsic velocity u and the momentum associated velocity \mathbf{v} as well as the temporal evolution of the fiber length L . The balance laws for mass and momentum combine the unrestricted motion and shape of the fiber center-line with the inner viscous transport and surface tension. Hence, they cover most of the previously derived models for nearly straight and curved stationary fibers as we will comment on in the following.

The one-dimensional stresses

$$\mathbf{s} = \mathbf{s}_{vis} + \mathbf{s}_{surf} = \left(\frac{3}{\text{Re}} A \partial_s u + \frac{\sqrt{\pi}}{2\text{We}} \sqrt{A} \right) \partial_s \boldsymbol{\gamma}$$

acting tangentially along the fiber stem from viscosity and surface tension, the first term particularly represents the Trouton viscosity [33]. Rewriting the dynamic boundary condition as $\mathbf{s}(L(t), t) = (\sqrt{\pi}/\text{We} \sqrt{A} \partial_s \boldsymbol{\gamma})(L(t), t)$ shows that the stresses at the fiber end balance the surface tension as in the full three-dimensional BVP. The temporal evolution of the bottom surface depends on the ratio of viscous forces and surface tension expressed by the capillary number $\text{Ca} = \text{We}/\text{Re}$. Using the conservation of mass and the boundary conditions it is particularly prescribed by the following initial value problem

$$\frac{dA(L(t), t)}{dt} = -(A \partial_s u)(L(t), t) = -\frac{\sqrt{\pi}}{6\text{Ca}} \sqrt{A}(L(t), t), \quad A(0, 0) = 1,$$

whose unique solution is

$$A(L(t), t) = \begin{cases} (1 - t/t_c)^2, & t \leq t_c \\ 0, & t > t_c \end{cases}, \quad t_c = \frac{12}{\sqrt{\pi}} \text{Ca}.$$

since $A \geq 0$. Thus, the behavior of the bottom surface is decoupled from the acting body forces whose specification closes the underlying free BVP. In the application of rotational spinning processes we deal with force densities \mathbf{f} coming from gravitation and rotation,

$$\mathbf{f} = \frac{1}{\text{Fr}^2} \mathbf{e}_g - \frac{2}{\text{Rb}} (\mathbf{e}_\omega \times \mathbf{v}) - \frac{1}{\text{Rb}^2} (\mathbf{e}_\omega \times (\mathbf{e}_\omega \times \boldsymbol{\gamma})).$$

where $g \mathbf{e}_g = \mathbf{g}$ denotes the acceleration of gravity and $\omega \mathbf{e}_\omega = \boldsymbol{\omega}$ the angular velocity of the rotating device. Thereby, the rotation axis goes through the origin. The dimensionless Froude $\text{Fr} = V/\sqrt{g\ell}$ and Rossby number $\text{Rb} = V/(\omega\ell)$ characterize the relation between inertial and gravitational forces, respectively between inertial and rotational forces.

To study the effects of surface tension, viscosity, gravitation and rotation on the fiber dynamics, we investigate the fiber behavior numerically by varying the characteristic numbers (We , Re , Fr and Rb). Therefore, we apply a finite volume method on a staggered grid with implicit upwind flux discretization. By adding a new cell per time step the increase of the length is realized, for details about the implementation we refer to [22].

4.1 Uniaxial Flow under Gravitation

Considering uniaxial flow under gravitation, our model simplifies to a system for A , u and L , but keeps the characteristics of the temporal evolution of the free fiber end:

$$\begin{aligned} \partial_t A + \partial_s (uA) &= 0 \\ \partial_t (Au) + \partial_s (u^2 A) &= \partial_s \left(\frac{3}{\text{Re}} A \partial_s u + \frac{\sqrt{\pi}}{2\text{We}} \sqrt{A} \right) + \frac{1}{\text{Fr}^2} A \end{aligned}$$

with the boundary conditions at the nozzle, $A(0, t) = 1$, $u(0, t) = 1$, and at the free end

$$\frac{dL(t)}{dt} = u(L(t), t), \quad L(0) = 0 \quad (A \partial_s u)(L(t), t) = \frac{\sqrt{\pi}}{6} \frac{\text{Re}}{\text{We}} \sqrt{A}(L(t), t)$$

Here, the geometry constraint and hence the variable $\boldsymbol{\gamma}$ vanish. Moreover, the momentum equation becomes scalar-valued, since the coupling condition results in $\mathbf{v} = u \mathbf{e}_g$ and the force densities reduce to $\mathbf{f} = \mathbf{e}_g/\text{Fr}^2$. For a fixed length and a pulling velocity applied at the fiber end, the balance laws are well-known in the context of glass fiber drawing processes, e.g. [3, 26, 25], and analyzed with regard to stability, e.g. [16, 17, 37]. Without surface tension the system has been applied for the

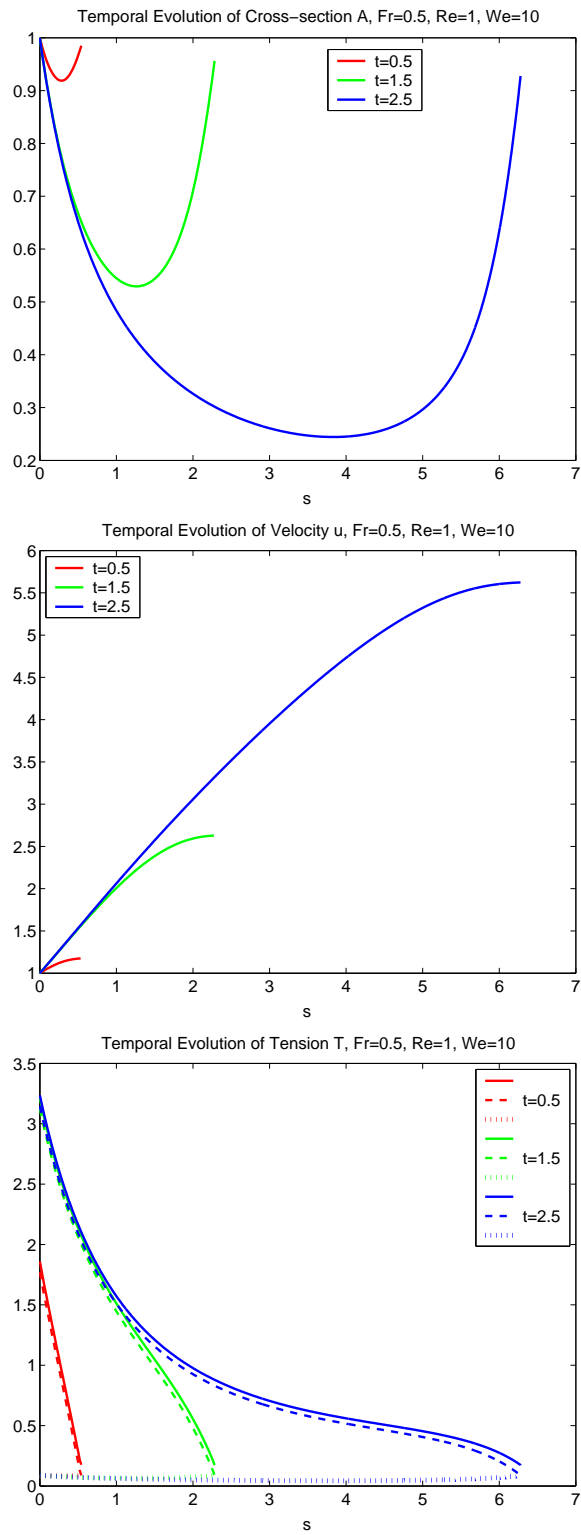


Figure 2: Top to bottom: Temporal evolution of A , u and stresses s (-), s_{vis} (-.), s_{surf} (:.) for uniaxial flow, $Fr=0.5$, $Re=1$, $We=10$

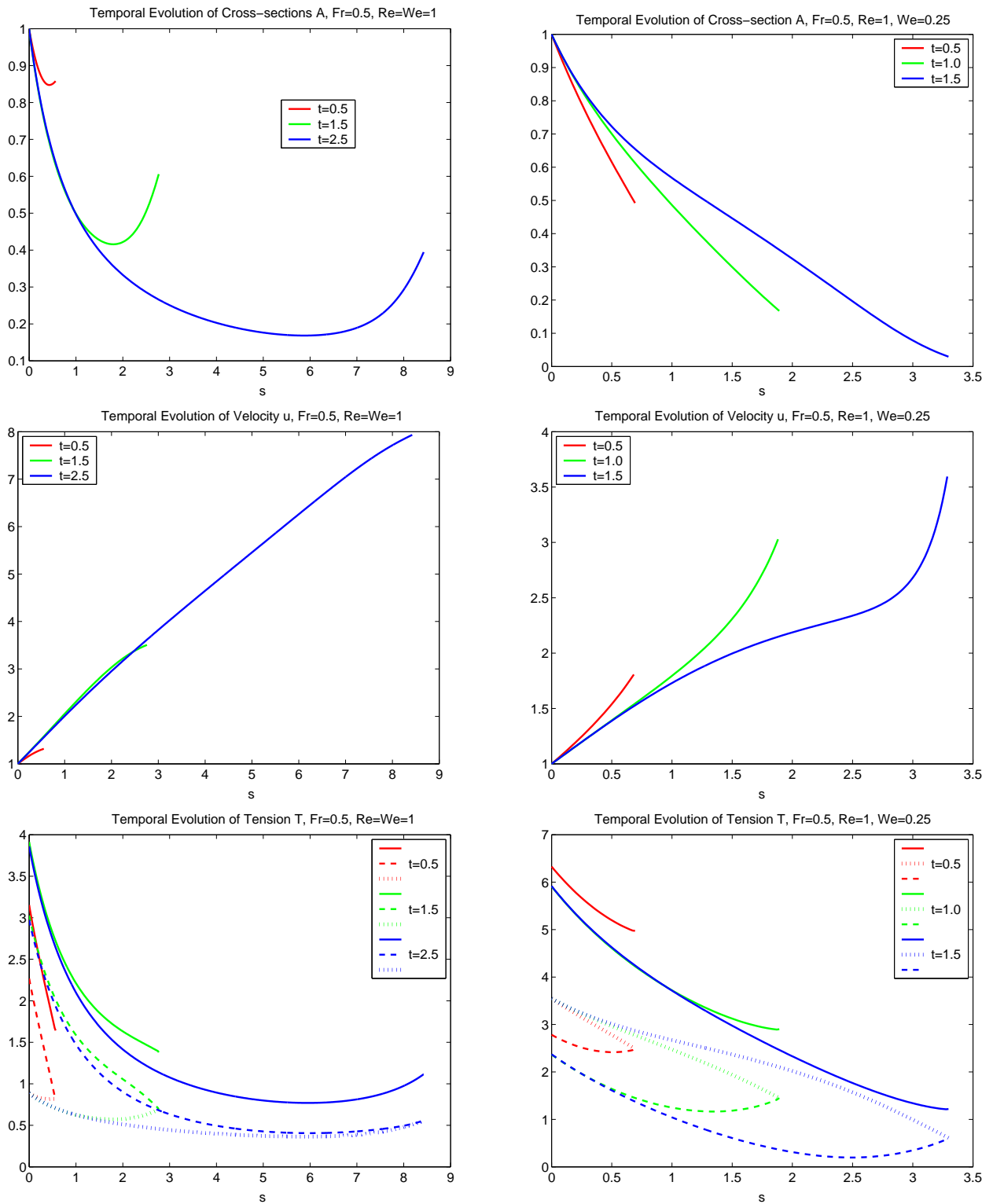


Figure 3: Top to bottom: Temporal evolution of A , u and stresses s (-), s_{vis} (-.), s_{surf} (:.) for uniaxial flow, $Fr=0.5$, $Re=1$. Left: $We=1$. Right: $We=0.25$

simulation of the extensional fall of viscous drops by using a finite element method in terms of a Lagrangian framework [31]. On the other hand, Panda [22] has developed a numerical scheme based on a finite volume method on a staggered grid in Eulerian coordinates that we have extended here appropriately. In the absence of surface tension, $We \rightarrow \infty$, our results coincide with [22, 31], where the bottom cross-section keeps the initial value $A(L(t), t) = A(0, 0)$ since $\partial_s u(L(t), t) = 0$. This effect occurs separately in a boundary layer and has almost no influence on the remaining fiber behavior, see Yarin [36] and Fig 2 for $We = 10$.

Figure 2 and 3 illustrate the temporal evolution of the fiber properties, i.e. cross-section A , velocity u and stresses s , for three different scenarios where Froude and Reynolds numbers are fixed $(Fr, Re) = (0.5, 1)$ and the Weber number varies $We \in \{0.25, 1, 10\}$. The lower the Weber number, the faster is the decrease of the bottom cross-section and the increase of the velocity. The scalar-valued tension s is dominated by the part stemming from the surface tension $s_{surf} = \sqrt{\pi A}/(2We)$, whereas the viscous tension $s_{vis} = 3A\partial_s u/Re$ drops rapidly down to zero. When the viscous stresses become negative due to a sign change of $\partial_s u$, the simulated model loses its validity according to Wong et.al. [35]. The higher the Weber numbers, the longer it takes to reach this critical point.

4.2 Curved Flow under Gravitation and Rotation

Analogously, three-dimensional flow under gravitation and rotation described by the full model can be studied numerically. For different scenarios Figures 4-6 show the temporal evolution for cross-section A , intrinsic velocity u and the projection of the fiber center-line in the \mathbf{e}_1 - \mathbf{e}_2 -plane that illustrates the curling behavior of the fiber. The simulation results we obtain for high Reynolds number flow coincide well with the parameter studies of [35, 34, 6]: the smaller the Rossby number, the higher the fiber curling. The curling is additionally influenced by the Weber number. Moreover, the magnitude of the Weber number determines the rate of thinning of the fiber ending as in the case of uniaxial flow. The time $t_c = 12We/(\sqrt{\pi}Re)$ when the fiber ending shrinks to a point is observed in the simulations. In contrast to [34, 6], our model enables the numerical simulation of the instationary fiber center-line for small Reynolds number flow, see e.g. Figures 5 and 1, which becomes important in the application of rotational glass spinning processes.

However note that the applicability of our model is restricted to certain parameter ranges. Physically relevant solutions for the model reduced to stationarity and $We \rightarrow \infty$ exist only for $Re^{-1} < Rb^2$, $Rb \rightarrow 0$, $Re \rightarrow \infty$, [18]. Including surface tension, the question of existence becomes even more delicate. Problems at the nozzle occur numerically for small Weber numbers. They are probably caused by a failure of the slender body theory at the nozzle, cf. [11]. This remains to be further investigated.

5 Conclusion

The one-dimensional model that we have asymptotically derived in this paper enables the simulation of instationary, curved, highly viscous fibers with surface tension and free ending as they occur in rotational spinning processes. The stated balance laws for mass and momentum are a generalization of many existing approaches, since they combine the unrestricted motion of the fiber center-line with inner transport and surface tension. The boundary condition shows the dependence of the temporal evolution of the free ending on the ratio of the viscous forces and the surface tension. The obtained numerical results are physically realistic except of the effects appearing at the nozzle for $Re^{-1} > Rb^2$ as well as for small We . These effects indicate the failure of the slender body theory due to the expected rise of a transition region. This phenomenon of "die swelling"

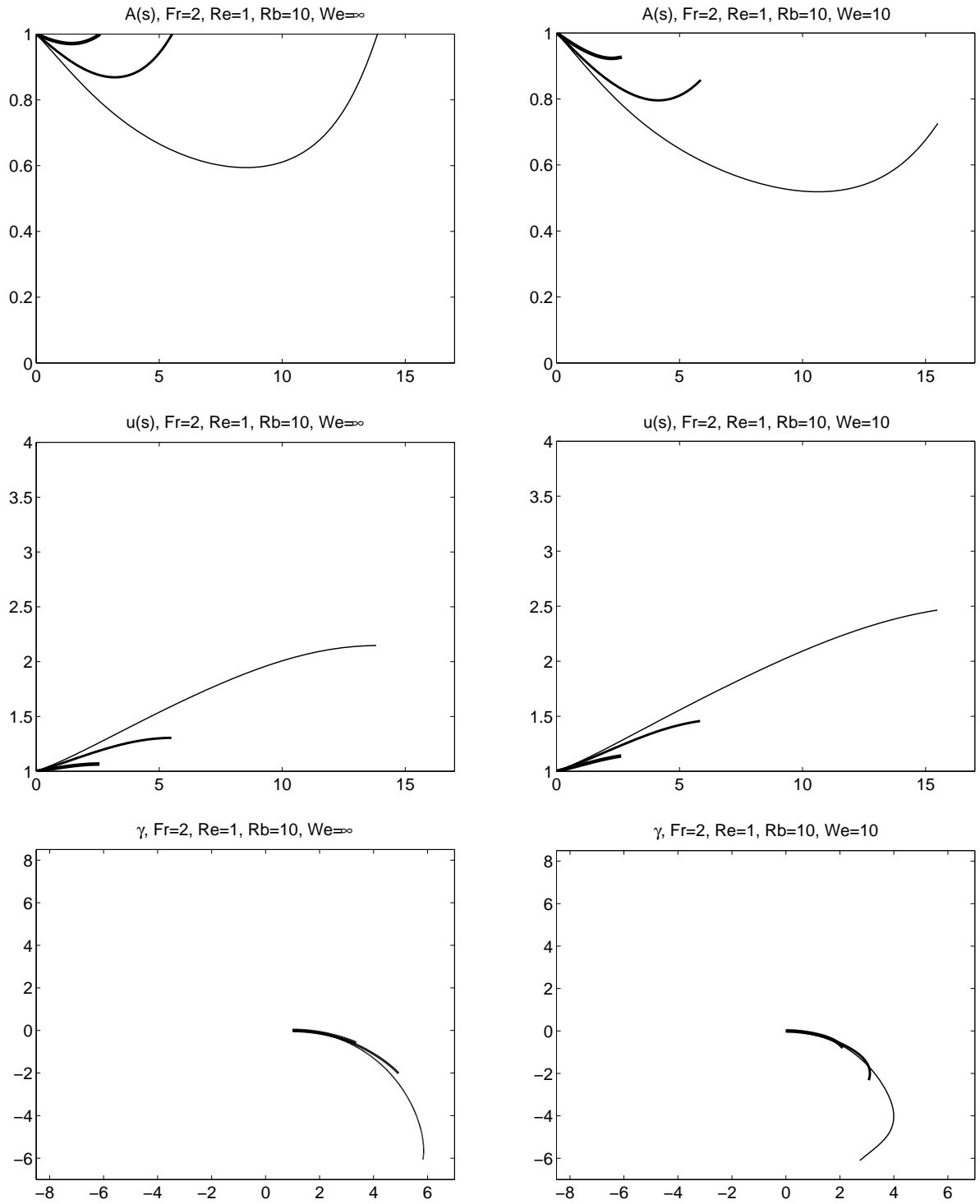


Figure 4: Top to bottom: Temporal evolution of A and u as well as of the projection of γ in \mathbf{e}_1 - \mathbf{e}_2 -plane, i.e. top view, for $t \in \{2.5, 5, 10\}$, $Fr = 2$, $Re = 1$, $Rb = 10$. Left: $We = \infty$. Right: $We = 10$.

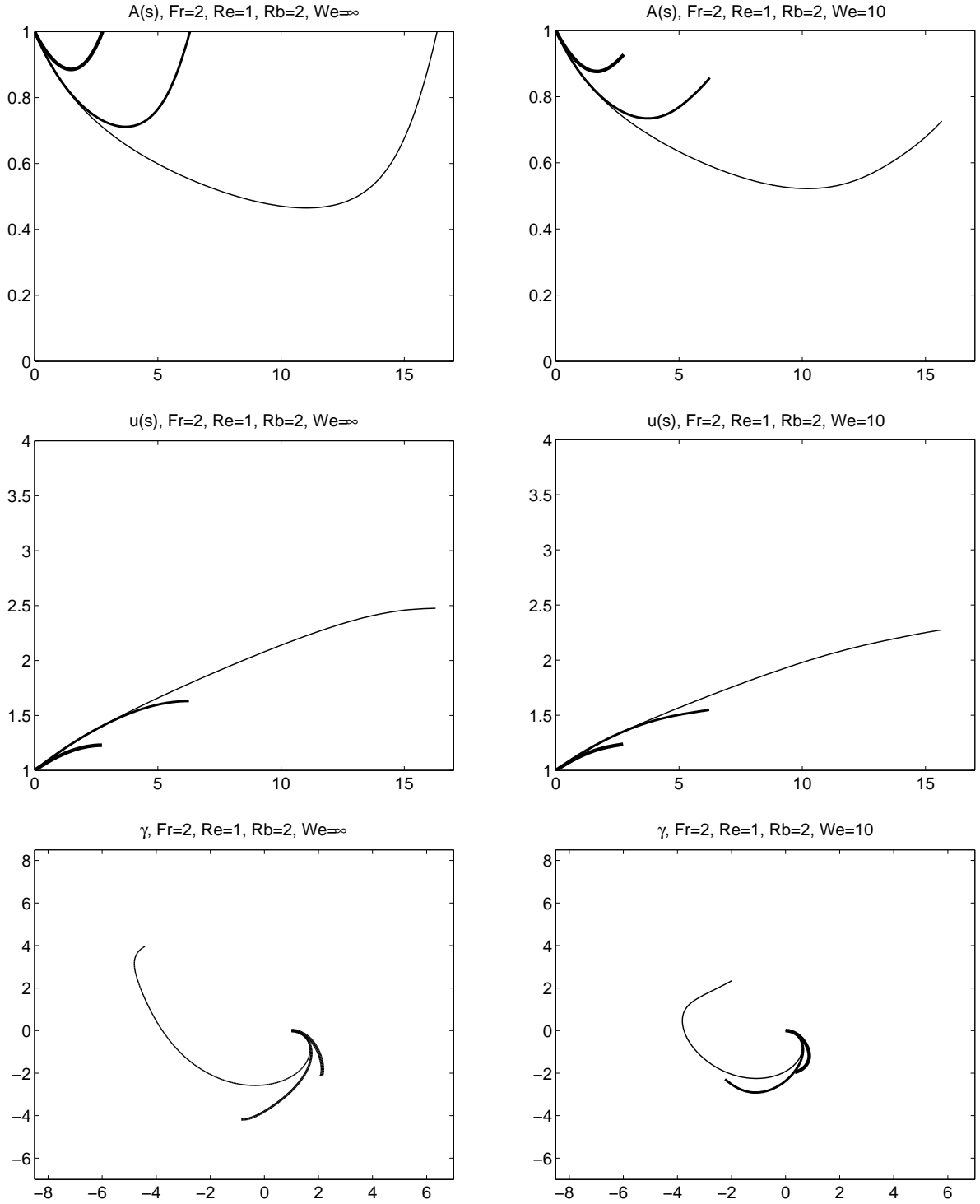


Figure 5: Top to bottom: Temporal evolution of A and u as well as of the projection of γ in \mathbf{e}_1 - \mathbf{e}_2 -plane, i.e. top view, for $t \in \{2.5, 5, 10\}$, $Fr = 2$, $Re = 1$, $Rb = 2$. Left: $We = \infty$. Right: $We = 10$.

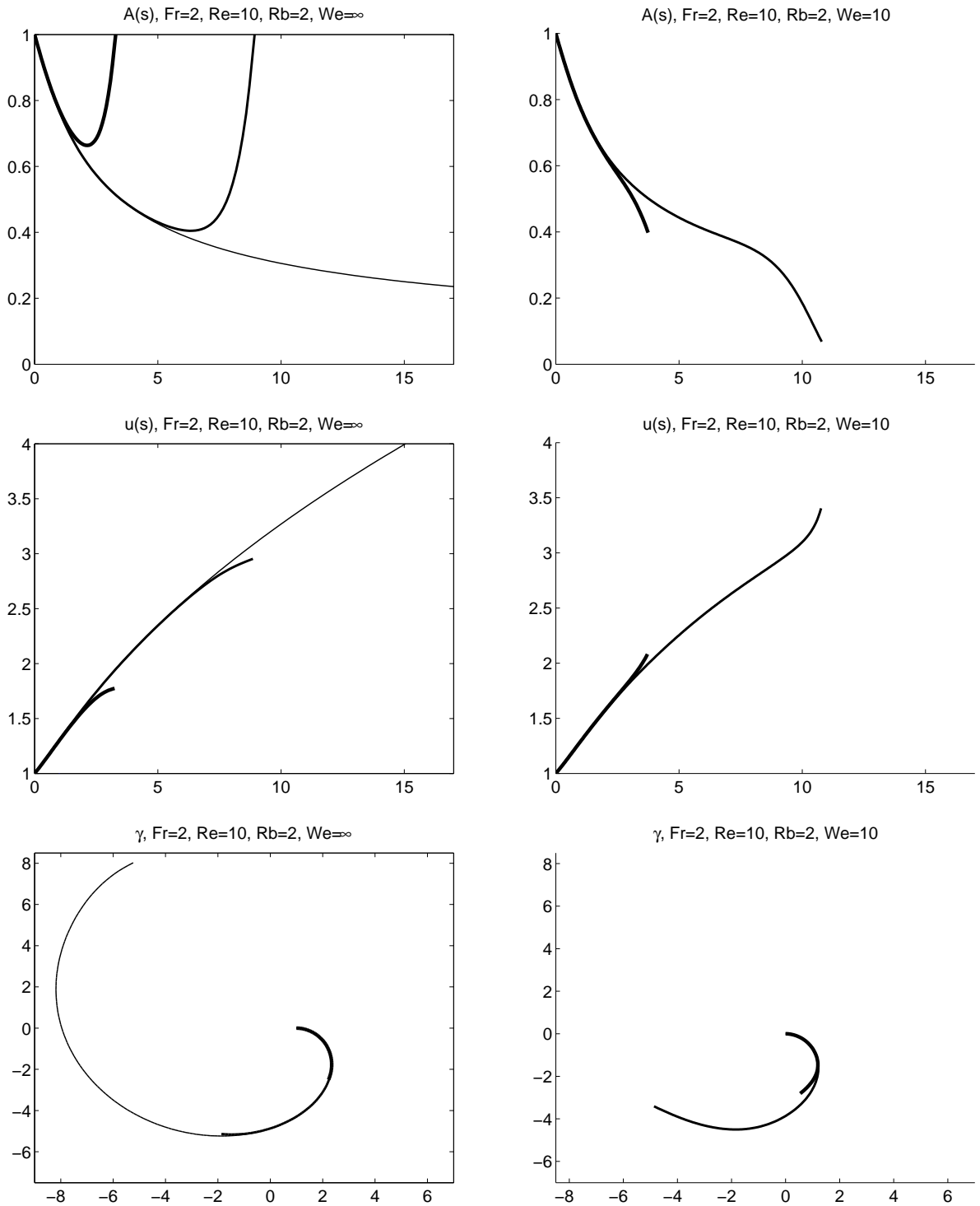


Figure 6: Top to bottom: Temporal evolution of A and u as well as of the projection of γ in \mathbf{e}_1 - \mathbf{e}_2 -plane, i.e. top view, $Fr = 2$, $Re = 10$, $Rb = 2$. Left: $We = \infty$ for $t \in \{2.5, 5, 10\}$. Right: $We = 10$ for $t \in \{2.5, 5\}$, note that $t_c = 6.8$.

requires further theoretical and numerical investigations. Numerical comparisons of the one- with the full three-dimensional model are therefore in preparation.

Acknowledgment

This work has been supported by the Kaiserslautern Excellence Cluster *Dependable Adaptive Systems and Mathematical Modeling*.

References

- [1] S. BECHTEL, M. FOREST, D. HOLM, AND K. LIN, *One-dimensional closure models for three-dimensional incompressible viscoelastic free jets: von karman flow geometry and elliptical cross-section*, JFM, 196 (1988), pp. 241–262.
- [2] R. BISHOP, *There is more than one way to frame a curve*, Amer Math Month, 82 (1975), pp. 246–251.
- [3] R. CAROSELLI, *Glass textile fibers*, in Man-Made Fibers, Science and Technology, H. Mark, S. Atlas, and C. E., eds., vol. 3, Interscience, New York, 1999, pp. 361–389.
- [4] L. CUMMINGS AND P. HOWELL, *On the evolution of non-axisymmetric viscous fibres with surface tension inertia and gravity*, JFM, 389 (1999), pp. 361–389.
- [5] S. DECENT, A. KING, AND I. WALLWORK, *Free jets spun from a prilling tower*, J Eng Math, 42 (2002), pp. 265–282.
- [6] S. DECENT, M. SIMMONS, E. PARAU, D. WONG, A. KING, AND L. PARTRIDGE, *Liquid jets from a rotating orifice*, in Proceedings of the 5th Int. Conf. on Multiphase Flow, ICMF’ 04, Yokohama, Japan, 2004.
- [7] J. DEWYNNE, P. HOWELL, AND P. WILMOTT, *Slender viscous fibers with inertia and gravity*, Quart J Mech Appl Math, 47 (1994), pp. 541–555.
- [8] J. DEWYNNE, J. OCKENDON, AND P. WILMOT, *A systematic derivation of the leading-order equations for extensional flows in slender geometries*, JFM, 244 (1992), pp. 323–338.
- [9] J. DEWYNNE AND P. WILMOTT, *Slender axisymmetric fluid jets*, Math Comp Model, 18 (1993), pp. 69–82.
- [10] M. DO CARMO, *Differentialgeometrie von Kurven und Flächen*, Vieweg, 1998.
- [11] J. EGGERS AND T. DUPONT, *Drop formation in a one-dimensional approximation of the Navier-Stokes equation*, JFM, 262 (2001), pp. 205–221.
- [12] V. ENTOV AND A. YARIN, *The dynamics of thin liquid jets in air*, JFM, 140 (1984), pp. 91–111.
- [13] M. FOREST AND Q. WANG, *Dynamics of slender viscoelastic free jets*, SIAM J Appl Math, 54 (1994), pp. 996–1032.
- [14] M. FOREST, Q. WANG, AND S. BECHTEL, *1d models for thin filaments of liquid crystalline polymers: Coupling of orientation and flow in the stability of simple solutions*, Physics D, 99 (2000), pp. 527–554.
- [15] M. FOREST AND H. ZHOU, *Unsteady analyses of thermal glass fibre drawing process*, EJAM, 12 (2001), pp. 497–496.
- [16] F. GEYLING AND G. HOMSEY, *Extensional instabilities of the glass fiber drawing process*, Glass Technol, 21 (1980), pp. 95–102.
- [17] P. GOSPODINOV AND V. ROUSSINOV, *Nonlinear instability during the isothermal drawing of optical fibers*, Int J Multiphase Flow, 19 (1993), pp. 1153–1158.
- [18] T. GÖTZ, A. KLAR, A. UNTERREITER, AND R. WEGENER, *Numerical evidence for the non-existence of solutions of the equations describing rational spinning*, Fraunhofer ITWM Bericht, 108 (2007).
- [19] P. HOWELL AND M. SIEGEL, *The evolution of a slender non-axisymmetric drop in an extensional flow*, JFM, 521 (2004), pp. 155–180.
- [20] P. D. HOWELL, *Extensional thin layer flows*, PhD thesis, St. Catherine’s College, Oxford, 1994.
- [21] M. MATOVICH AND J. PEARSON, *Spinning a molten threadline. Steady-state isothermal viscous flows*, Ind Eng Chem Fundam, 8 (1969), p. 512.
- [22] S. PANDA, *The dynamics of viscous fibers*, PhD thesis, Technische Universität Kaiserslautern, 2006.
- [23] S. PANDA, R. WEGENER, AND N. MARHEINEKE, *Slender body theory for the dynamics of curved viscous fibers*, Berichte des Fraunhofer ITWM, 86 (2006).

- [24] L. PARTRIDGE, D. WONG, M. SIMMONS, E. PARAU, AND S. DECENT, *Experimental and theoretical description of the break up of curved liquid jets in the prilling process*, Chem Eng Res Des, 83, A11 (2005), pp. 1267–1275.
- [25] J. PEARSON, *Mechanics of polymer processing*, Elsevier, 1985.
- [26] J. PEARSON AND M. MATOVICH, *Spinning a molten threadline. Stability*, Ind Eng Chem Fundam, 8 (1969), pp. 605–609.
- [27] N. RIBE, *Coiling of viscous jets*, PRS London, A 2051 (2004), pp. 3223–3239.
- [28] W. SCHULTZ AND S. DAVIS, *One-dimensional liquid fibres*, J Rheology, 26 (1982), pp. 331–345.
- [29] F. SHAH AND J. PEARSON, *On the stability of non-isothermal fibre spinning*, Ind Eng Chem Fundam, 11 (1972), pp. 145–149.
- [30] A. SIEROU AND J. LISTER, *Self-similar solutions for viscous capillary pinch-off*, JFM, 497 (2003), pp. 381–403.
- [31] Y. STOKES AND E. TUCK, *The role of inertia in extensional fall of viscous drop*, JFM, 498 (2004), pp. 205–225.
- [32] Y. STOKES, E. TUCK, AND L. SCHWARTZ, *Extensional fall of a very viscous fluid drop*, Quart J Mech Appl Math, 53 (2000), pp. 565–582.
- [33] F. R. S. TROUTON, *On the coefficient of viscous traction and its relation to that of viscosity*, PRS London, A 77 (1906), pp. 426–440.
- [34] I. M. WALLWORK, S. P. DECENT, A. C. KING, AND F. R. S. SCHULKES, R. M. S. M. TROUTON, *The trajectory and stability of a spiralling liquid jet. Part 1. Inviscid theory*, JFM, 459 (2002), pp. 43–65.
- [35] D. WONG, M. SIMMONS, S. DECENT, E. PARAU, AND A. KING, *Break up dynamics and drop size distributions created from curved liquid jets*, Int J Multiphase Flow, 30 (2004), pp. 499–520.
- [36] A. YARIN, *Free liquid jets and films: Hydrodynamics and rheology*, Longman, New York, 1993.
- [37] A. YARIN, P. GOSPODINOV, O. GOTTLIEB, AND M. GRAHAM, *Newtonian glass fiber drawing: Chaotic variation of the cross-sectional radius*, Phys Fluids, 11 (1999), pp. 3201–3208.

Published reports of the Fraunhofer ITWM

The PDF-files of the following reports are available under:

www.itwm.fraunhofer.de/de/zentral__berichte/berichte

1. D. Hietel, K. Steiner, J. Struckmeier
A Finite - Volume Particle Method for Compressible Flows
(19 pages, 1998)
2. M. Feldmann, S. Seibold
Damage Diagnosis of Rotors: Application of Hilbert Transform and Multi-Hypothesis Testing
Keywords: Hilbert transform, damage diagnosis, Kalman filtering, non-linear dynamics
(23 pages, 1998)
3. Y. Ben-Haim, S. Seibold
Robust Reliability of Diagnostic Multi-Hypothesis Algorithms: Application to Rotating Machinery
Keywords: Robust reliability, convex models, Kalman filtering, multi-hypothesis diagnosis, rotating machinery, crack diagnosis
(24 pages, 1998)
4. F.-Th. Lentjes, N. Siedow
Three-dimensional Radiative Heat Transfer in Glass Cooling Processes
(23 pages, 1998)
5. A. Klar, R. Wegener
A hierarchy of models for multilane vehicular traffic
Part I: Modeling
(23 pages, 1998)

Part II: Numerical and stochastic investigations
(17 pages, 1998)
6. A. Klar, N. Siedow
Boundary Layers and Domain Decomposition for Radiative Heat Transfer and Diffusion Equations: Applications to Glass Manufacturing Processes
(24 pages, 1998)
7. I. Choquet
Heterogeneous catalysis modelling and numerical simulation in rarified gas flows
Part I: Coverage locally at equilibrium
(24 pages, 1998)
8. J. Ohser, B. Steinbach, C. Lang
Efficient Texture Analysis of Binary Images
(17 pages, 1998)
9. J. Orlik
Homogenization for viscoelasticity of the integral type with aging and shrinkage
(20 pages, 1998)
10. J. Mohring
Helmholtz Resonators with Large Aperture
(21 pages, 1998)
11. H. W. Hamacher, A. Schöbel
On Center Cycles in Grid Graphs
(15 pages, 1998)
12. H. W. Hamacher, K.-H. Küfer
Inverse radiation therapy planning - a multiple objective optimisation approach
(14 pages, 1999)
13. C. Lang, J. Ohser, R. Hilfer
On the Analysis of Spatial Binary Images
(20 pages, 1999)
14. M. Junk
On the Construction of Discrete Equilibrium Distributions for Kinetic Schemes
(24 pages, 1999)
15. M. Junk, S. V. Raghurame Rao
A new discrete velocity method for Navier-Stokes equations
(20 pages, 1999)
16. H. Neunzert
Mathematics as a Key to Key Technologies
(39 pages (4 PDF-Files), 1999)
17. J. Ohser, K. Sandau
Considerations about the Estimation of the Size Distribution in Wicksell's Corpuscle Problem
(18 pages, 1999)
18. E. Carrizosa, H. W. Hamacher, R. Klein, S. Nickel
Solving nonconvex planar location problems by finite dominating sets
Keywords: Continuous Location, Polyhedral Gauges, Finite Dominating Sets, Approximation, Sandwich Algorithm, Greedy Algorithm
(19 pages, 2000)
19. A. Becker
A Review on Image Distortion Measures
Keywords: Distortion measure, human visual system
(26 pages, 2000)
20. H. W. Hamacher, M. Labbé, S. Nickel, T. Sonneborn
Polyhedral Properties of the Uncapacitated Multiple Allocation Hub Location Problem
Keywords: integer programming, hub location, facility location, valid inequalities, facets, branch and cut
(21 pages, 2000)
21. H. W. Hamacher, A. Schöbel
Design of Zone Tariff Systems in Public Transportation
(30 pages, 2001)
22. D. Hietel, M. Junk, R. Keck, D. Teleaga
The Finite-Volume-Particle Method for Conservation Laws
(16 pages, 2001)
23. T. Bender, H. Hennes, J. Kalcsics, M. T. Melo, S. Nickel
Location Software and Interface with GIS and Supply Chain Management
Keywords: facility location, software development, geographical information systems, supply chain management
(48 pages, 2001)
24. H. W. Hamacher, S. A. Tjandra
Mathematical Modelling of Evacuation Problems: A State of Art
(44 pages, 2001)
25. J. Kuhnert, S. Tiwari
Grid free method for solving the Poisson equation
Keywords: Poisson equation, Least squares method, Grid free method
(19 pages, 2001)
26. T. Götz, H. Rave, D. Reinel-Bitzer, K. Steiner, H. Tiemeier
Simulation of the fiber spinning process
Keywords: Melt spinning, fiber model, Lattice Boltzmann, CFD
(19 pages, 2001)
27. A. Zemitis
On interaction of a liquid film with an obstacle
Keywords: impinging jets, liquid film, models, numerical solution, shape
(22 pages, 2001)
28. I. Ginzburg, K. Steiner
Free surface lattice-Boltzmann method to model the filling of expanding cavities by Bingham Fluids
Keywords: Generalized LBE, free-surface phenomena, interface boundary conditions, filling processes, Bingham viscoplastic model, regularized models
(22 pages, 2001)
29. H. Neunzert
»Denn nichts ist für den Menschen als Menschen etwas wert, was er nicht mit Leidenschaft tun kann«
Vortrag anlässlich der Verleihung des Akademiepreises des Landes Rheinland-Pfalz am 21.11.2001
Keywords: Lehre, Forschung, angewandte Mathematik, Mehrskalalanalyse, Strömungsmechanik
(18 pages, 2001)
30. J. Kuhnert, S. Tiwari
Finite pointset method based on the projection method for simulations of the incompressible Navier-Stokes equations
Keywords: Incompressible Navier-Stokes equations, Meshfree method, Projection method, Particle scheme, Least squares approximation
AMS subject classification: 76D05, 76M28
(25 pages, 2001)
31. R. Korn, M. Krekel
Optimal Portfolios with Fixed Consumption or Income Streams
Keywords: Portfolio optimisation, stochastic control, HJB equation, discretisation of control problems.
(23 pages, 2002)
32. M. Krekel
Optimal portfolios with a loan dependent credit spread
Keywords: Portfolio optimisation, stochastic control, HJB equation, credit spread, log utility, power utility, non-linear wealth dynamics
(25 pages, 2002)
33. J. Ohser, W. Nagel, K. Schladitz
The Euler number of discretized sets – on the choice of adjacency in homogeneous lattices
Keywords: image analysis, Euler number, neighborhood relationships, cuboidal lattice
(32 pages, 2002)

34. I. Ginzburg, K. Steiner
Lattice Boltzmann Model for Free-Surface flow and Its Application to Filling Process in Casting
Keywords: Lattice Boltzmann models; free-surface phenomena; interface boundary conditions; filling processes; injection molding; volume of fluid method; interface boundary conditions; advection-schemes; up-wind-schemes (54 pages, 2002)
35. M. Günther, A. Klar, T. Materne, R. Wegener
Multivalued fundamental diagrams and stop and go waves for continuum traffic equations
Keywords: traffic flow, macroscopic equations, kinetic derivation, multivalued fundamental diagram, stop and go waves, phase transitions (25 pages, 2002)
36. S. Feldmann, P. Lang, D. Prätzel-Wolters
Parameter influence on the zeros of network determinants
Keywords: Networks, Equicofactor matrix polynomials, Realization theory, Matrix perturbation theory (30 pages, 2002)
37. K. Koch, J. Ohser, K. Schladitz
Spectral theory for random closed sets and estimating the covariance via frequency space
Keywords: Random set, Bartlett spectrum, fast Fourier transform, power spectrum (28 pages, 2002)
38. D. d'Humières, I. Ginzburg
Multi-reflection boundary conditions for lattice Boltzmann models
Keywords: lattice Boltzmann equation, boundary conditions, bounce-back rule, Navier-Stokes equation (72 pages, 2002)
39. R. Korn
Elementare Finanzmathematik
Keywords: Finanzmathematik, Aktien, Optionen, Portfolio-Optimierung, Börse, Lehrerweiterbildung, Mathematikunterricht (98 pages, 2002)
40. J. Kallrath, M. C. Müller, S. Nickel
Batch Presorting Problems: Models and Complexity Results
Keywords: Complexity theory, Integer programming, Assignment, Logistics (19 pages, 2002)
41. J. Linn
On the frame-invariant description of the phase space of the Folgar-Tucker equation
Key words: fiber orientation, Folgar-Tucker equation, injection molding (5 pages, 2003)
42. T. Hanne, S. Nickel
A Multi-Objective Evolutionary Algorithm for Scheduling and Inspection Planning in Software Development Projects
Key words: multiple objective programming, project management and scheduling, software development, evolutionary algorithms, efficient set (29 pages, 2003)
43. T. Bortfeld, K.-H. Küfer, M. Monz, A. Scherrer, C. Thieke, H. Trinkaus
Intensity-Modulated Radiotherapy - A Large Scale Multi-Criteria Programming Problem
Keywords: multiple criteria optimization, representative systems of Pareto solutions, adaptive triangulation, clustering and disaggregation techniques, visualization of Pareto solutions, medical physics, external beam radiotherapy planning, intensity modulated radiotherapy (31 pages, 2003)
44. T. Halfmann, T. Wichmann
Overview of Symbolic Methods in Industrial Analog Circuit Design
Keywords: CAD, automated analog circuit design, symbolic analysis, computer algebra, behavioral modeling, system simulation, circuit sizing, macro modeling, differential-algebraic equations, index (17 pages, 2003)
45. S. E. Mikhailov, J. Orlik
Asymptotic Homogenisation in Strength and Fatigue Durability Analysis of Composites
Keywords: multiscale structures, asymptotic homogenization, strength, fatigue, singularity, non-local conditions (14 pages, 2003)
46. P. Domínguez-Marín, P. Hansen, N. Mladenović, S. Nickel
Heuristic Procedures for Solving the Discrete Ordered Median Problem
Keywords: genetic algorithms, variable neighborhood search, discrete facility location (31 pages, 2003)
47. N. Boland, P. Domínguez-Marín, S. Nickel, J. Puerto
Exact Procedures for Solving the Discrete Ordered Median Problem
Keywords: discrete location, Integer programming (41 pages, 2003)
48. S. Feldmann, P. Lang
Padé-like reduction of stable discrete linear systems preserving their stability
Keywords: Discrete linear systems, model reduction, stability, Hankel matrix, Stein equation (16 pages, 2003)
49. J. Kallrath, S. Nickel
A Polynomial Case of the Batch Presorting Problem
Keywords: batch presorting problem, online optimization, competitive analysis, polynomial algorithms, logistics (17 pages, 2003)
50. T. Hanne, H. L. Trinkaus
knowCube for MCDM – Visual and Interactive Support for Multicriteria Decision Making
Key words: Multicriteria decision making, knowledge management, decision support systems, visual interfaces, interactive navigation, real-life applications. (26 pages, 2003)
51. O. Iliev, V. Laptev
On Numerical Simulation of Flow Through Oil Filters
Keywords: oil filters, coupled flow in plain and porous media, Navier-Stokes, Brinkman, numerical simulation (8 pages, 2003)
52. W. Dörfler, O. Iliev, D. Stoyanov, D. Vassileva
On a Multigrid Adaptive Refinement Solver for Saturated Non-Newtonian Flow in Porous Media
Keywords: Nonlinear multigrid, adaptive refinement, Heston model, stochastic volatility, cliquet options (17 pages, 2003)
53. S. Kruse
On the Pricing of Forward Starting Options under Stochastic Volatility
Keywords: Option pricing, forward starting options, Heston model, stochastic volatility, cliquet options (11 pages, 2003)
54. O. Iliev, D. Stoyanov
Multigrid – adaptive local refinement solver for incompressible flows
Keywords: Navier-Stokes equations, incompressible flow, projection-type splitting, SIMPLE, multigrid methods, adaptive local refinement, lid-driven flow in a cavity (37 pages, 2003)
55. V. Starikovicius
The multiphase flow and heat transfer in porous media
Keywords: Two-phase flow in porous media, various formulations, global pressure, multiphase mixture model, numerical simulation (30 pages, 2003)
56. P. Lang, A. Sarishvili, A. Wirsén
Blocked neural networks for knowledge extraction in the software development process
Keywords: Blocked Neural Networks, Nonlinear Regression, Knowledge Extraction, Code Inspection (21 pages, 2003)
57. H. Knaf, P. Lang, S. Zeiser
Diagnosis aiding in Regulation Thermography using Fuzzy Logic
Keywords: fuzzy logic, knowledge representation, expert system (22 pages, 2003)
58. M. T. Melo, S. Nickel, F. Saldanha da Gama
Largescale models for dynamic multi-commodity capacitated facility location
Keywords: supply chain management, strategic planning, dynamic location, modeling (40 pages, 2003)
59. J. Orlik
Homogenization for contact problems with periodically rough surfaces
Keywords: asymptotic homogenization, contact problems (28 pages, 2004)
60. A. Scherrer, K.-H. Küfer, M. Monz, F. Alonso, T. Bortfeld
IMRT planning on adaptive volume structures – a significant advance of computational complexity
Keywords: Intensity-modulated radiation therapy (IMRT), inverse treatment planning, adaptive volume structures, hierarchical clustering, local refinement, adaptive clustering, convex programming, mesh generation, multi-grid methods (24 pages, 2004)

61. D. Kehrwald
Parallel lattice Boltzmann simulation of complex flows
Keywords: Lattice Boltzmann methods, parallel computing, microstructure simulation, virtual material design, pseudo-plastic fluids, liquid composite moulding (12 pages, 2004)
62. O. Iliev, J. Linn, M. Moog, D. Niedziela, V. Starikovicus
On the Performance of Certain Iterative Solvers for Coupled Systems Arising in Discretization of Non-Newtonian Flow Equations
Keywords: Performance of iterative solvers, Preconditioners, Non-Newtonian flow (17 pages, 2004)
63. R. Ciegis, O. Iliev, S. Rief, K. Steiner
On Modelling and Simulation of Different Regimes for Liquid Polymer Moulding
Keywords: Liquid Polymer Moulding, Modelling, Simulation, Infiltration, Front Propagation, non-Newtonian flow in porous media (43 pages, 2004)
64. T. Hanne, H. Neu
Simulating Human Resources in Software Development Processes
Keywords: Human resource modeling, software process, productivity, human factors, learning curve (14 pages, 2004)
65. O. Iliev, A. Mikelic, P. Popov
Fluid structure interaction problems in deformable porous media: Toward permeability of deformable porous media
Keywords: fluid-structure interaction, deformable porous media, upscaling, linear elasticity, stokes, finite elements (28 pages, 2004)
66. F. Gaspar, O. Iliev, F. Lisbona, A. Naumovich, P. Vabishchevich
On numerical solution of 1-D poroelasticity equations in a multilayered domain
Keywords: poroelasticity, multilayered material, finite volume discretization, MAC type grid (41 pages, 2004)
67. J. Ohser, K. Schladitz, K. Koch, M. Nöthe
Diffraction by image processing and its application in materials science
Keywords: porous microstructure, image analysis, random set, fast Fourier transform, power spectrum, Bartlett spectrum (13 pages, 2004)
68. H. Neunzert
Mathematics as a Technology: Challenges for the next 10 Years
Keywords: applied mathematics, technology, modelling, simulation, visualization, optimization, glass processing, spinning processes, fiber-fluid interaction, turbulence effects, topological optimization, multicriteria optimization, Uncertainty and Risk, financial mathematics, Malliavin calculus, Monte-Carlo methods, virtual material design, filtration, bio-informatics, system biology (29 pages, 2004)
69. R. Ewing, O. Iliev, R. Lazarov, A. Naumovich
On convergence of certain finite difference discretizations for 1D poroelasticity interface problems
Keywords: poroelasticity, multilayered material, finite volume discretizations, MAC type grid, error estimates (26 pages, 2004)
70. W. Dörfler, O. Iliev, D. Stoyanov, D. Vassileva
On Efficient Simulation of Non-Newtonian Flow in Saturated Porous Media with a Multigrid Adaptive Refinement Solver
Keywords: Nonlinear multigrid, adaptive refinement, non-Newtonian in porous media (25 pages, 2004)
71. J. Kalcsics, S. Nickel, M. Schröder
Towards a Unified Territory Design Approach – Applications, Algorithms and GIS Integration
Keywords: territory design, political districting, sales territory alignment, optimization algorithms, Geographical Information Systems (40 pages, 2005)
72. K. Schladitz, S. Peters, D. Reinel-Bitzer, A. Wiegmann, J. Ohser
Design of acoustic trim based on geometric modeling and flow simulation for non-woven
Keywords: random system of fibers, Poisson line process, flow resistivity, acoustic absorption, Lattice-Boltzmann method, non-woven (21 pages, 2005)
73. V. Rutka, A. Wiegmann
Explicit Jump Immersed Interface Method for virtual material design of the effective elastic moduli of composite materials
Keywords: virtual material design, explicit jump immersed interface method, effective elastic moduli, composite materials (22 pages, 2005)
74. T. Hanne
Eine Übersicht zum Scheduling von Baustellen
Keywords: Projektplanung, Scheduling, Bauplanung, Bauindustrie (32 pages, 2005)
75. J. Linn
The Folgar-Tucker Model as a Differential Algebraic System for Fiber Orientation Calculation
Keywords: fiber orientation, Folgar-Tucker model, invariants, algebraic constraints, phase space, trace stability (15 pages, 2005)
76. M. Speckert, K. Dreßler, H. Mauch, A. Lion, G. J. Wierda
Simulation eines neuartigen Prüfsystems für Achserproben durch MKS-Modellierung einschließlich Regelung
Keywords: virtual test rig, suspension testing, multi-body simulation, modeling hexapod test rig, optimization of test rig configuration (20 pages, 2005)
77. K.-H. Küfer, M. Monz, A. Scherrer, P. Süß, F. Alonso, A. S. A. Sultan, Th. Bortfeld, D. Craft, Chr. Thieke
Multicriteria optimization in intensity modulated radiotherapy planning
Keywords: multicriteria optimization, extreme solutions, real-time decision making, adaptive approximation schemes, clustering methods, IMRT planning, reverse engineering (51 pages, 2005)
78. S. Amstutz, H. Andrä
A new algorithm for topology optimization using a level-set method
Keywords: shape optimization, topology optimization, topological sensitivity, level-set (22 pages, 2005)
79. N. Ettrich
Generation of surface elevation models for urban drainage simulation
Keywords: Flooding, simulation, urban elevation models, laser scanning (22 pages, 2005)
80. H. Andrä, J. Linn, I. Matei, I. Shklyar, K. Steiner, E. Teichmann
OPTCAST – Entwicklung adäquater Strukturoptimierungsverfahren für Gießereien Technischer Bericht (KURZFASSUNG)
Keywords: Topologieoptimierung, Level-Set-Methode, Gießprozesssimulation, Gießtechnische Restriktionen, CAE-Kette zur Strukturoptimierung (77 pages, 2005)
81. N. Marheineke, R. Wegener
Fiber Dynamics in Turbulent Flows Part I: General Modeling Framework
Keywords: fiber-fluid interaction; Cosserat rod; turbulence modeling; Kolmogorov's energy spectrum; double-velocity correlations; differentiable Gaussian fields (20 pages, 2005)
Part II: Specific Taylor Drag
Keywords: flexible fibers; $k-\epsilon$ turbulence model; fiber-turbulence interaction scales; air drag; random Gaussian aerodynamic force; white noise; stochastic differential equations; ARMA process (18 pages, 2005)
82. C. H. Lampert, O. Wirjadi
An Optimal Non-Orthogonal Separation of the Anisotropic Gaussian Convolution Filter
Keywords: Anisotropic Gaussian filter, linear filtering, orientation space, nD image processing, separable filters (25 pages, 2005)
83. H. Andrä, D. Stoyanov
Error indicators in the parallel finite element solver for linear elasticity DDFEM
Keywords: linear elasticity, finite element method, hierarchical shape functions, domain decomposition, parallel implementation, a posteriori error estimates (21 pages, 2006)
84. M. Schröder, I. Solchenbach
Optimization of Transfer Quality in Regional Public Transit
Keywords: public transit, transfer quality, quadratic assignment problem (16 pages, 2006)
85. A. Naumovich, F. J. Gaspar
On a multigrid solver for the three-dimensional Biot poroelasticity system in multilayered domains
Keywords: poroelasticity, interface problem, multigrid, operator-dependent prolongation (11 pages, 2006)
86. S. Panda, R. Wegener, N. Marheineke
Slender Body Theory for the Dynamics of Curved Viscous Fibers
Keywords: curved viscous fibers; fluid dynamics; Navier-Stokes equations; free boundary value problem; asymptotic expansions; slender body theory (14 pages, 2006)
87. E. Ivanov, H. Andrä, A. Kudryavtsev
Domain Decomposition Approach for Automatic Parallel Generation of Tetrahedral Grids
Keywords: Grid Generation, Unstructured Grid, Delaunay Triangulation, Parallel Programming, Domain Decomposition, Load Balancing (18 pages, 2006)

88. S. Tiwari, S. Antonov, D. Hietel, J. Kuhnert, R. Wegener
A Meshfree Method for Simulations of Interactions between Fluids and Flexible Structures
Key words: Meshfree Method, FPM, Fluid Structure Interaction, Sheet of Paper, Dynamical Coupling (16 pages, 2006)
89. R. Ciegis, O. Iliev, V. Starikovicius, K. Steiner
Numerical Algorithms for Solving Problems of Multiphase Flows in Porous Media
Keywords: nonlinear algorithms, finite-volume method, software tools, porous media, flows (16 pages, 2006)
90. D. Niedziela, O. Iliev, A. Latz
On 3D Numerical Simulations of Viscoelastic Fluids
Keywords: non-Newtonian fluids, anisotropic viscosity, integral constitutive equation (18 pages, 2006)
91. A. Winterfeld
Application of general semi-infinite Programming to Lapidary Cutting Problems
Keywords: large scale optimization, nonlinear programming, general semi-infinite optimization, design centering, clustering (26 pages, 2006)
92. J. Orlik, A. Ostrovska
Space-Time Finite Element Approximation and Numerical Solution of Hereditary Linear Viscoelasticity Problems
Keywords: hereditary viscoelasticity; kern approximation by interpolation; space-time finite element approximation, stability and a priori estimate (24 pages, 2006)
93. V. Rutka, A. Wiegmann, H. Andrä
EJIM for Calculation of effective Elastic Moduli in 3D Linear Elasticity
Keywords: Elliptic PDE, linear elasticity, irregular domain, finite differences, fast solvers, effective elastic moduli (24 pages, 2006)
94. A. Wiegmann, A. Zemitis
EJ-HEAT: A Fast Explicit Jump Harmonic Averaging Solver for the Effective Heat Conductivity of Composite Materials
Keywords: Stationary heat equation, effective thermal conductivity, explicit jump, discontinuous coefficients, virtual material design, microstructure simulation, EJ-HEAT (21 pages, 2006)
95. A. Naumovich
On a finite volume discretization of the three-dimensional Biot poroelasticity system in multilayered domains
Keywords: Biot poroelasticity system, interface problems, finite volume discretization, finite difference method. (21 pages, 2006)
96. M. Krekel, J. Wenzel
A unified approach to Credit Default Swaption and Constant Maturity Credit Default Swap valuation
Keywords: LIBOR market model, credit risk, Credit Default Swaption, Constant Maturity Credit Default Swap-method. (43 pages, 2006)
97. A. Dreyer
Interval Methods for Analog Circuits
Keywords: interval arithmetic, analog circuits, tolerance analysis, parametric linear systems, frequency response, symbolic analysis, CAD, computer algebra (36 pages, 2006)
98. N. Weigel, S. Weihe, G. Bitsch, K. Dreßler
Usage of Simulation for Design and Optimization of Testing
Keywords: Vehicle test rigs, MBS, control, hydraulics, testing philosophy (14 pages, 2006)
99. H. Lang, G. Bitsch, K. Dreßler, M. Speckert
Comparison of the solutions of the elastic and elastoplastic boundary value problems
Keywords: Elastic BVP, elastoplastic BVP, variational inequalities, rate-independency, hysteresis, linear kinematic hardening, stop- and play-operator (21 pages, 2006)
100. M. Speckert, K. Dreßler, H. Mauch
MBS Simulation of a hexapod based suspension test rig
Keywords: Test rig, MBS simulation, suspension, hydraulics, controlling, design optimization (12 pages, 2006)
101. S. Azizi Sultan, K.-H. Küfer
A dynamic algorithm for beam orientations in multicriteria IMRT planning
Keywords: radiotherapy planning, beam orientation optimization, dynamic approach, evolutionary algorithm, global optimization (14 pages, 2006)
102. T. Götz, A. Klar, N. Marheineke, R. Wegener
A Stochastic Model for the Fiber Lay-down Process in the Nonwoven Production
Keywords: fiber dynamics, stochastic Hamiltonian system, stochastic averaging (17 pages, 2006)
103. Ph. Süß, K.-H. Küfer
Balancing control and simplicity: a variable aggregation method in intensity modulated radiation therapy planning
Keywords: IMRT planning, variable aggregation, clustering methods (22 pages, 2006)
104. A. Beaudry, G. Laporte, T. Melo, S. Nickel
Dynamic transportation of patients in hospitals
Keywords: in-house hospital transportation, dial-a-ride, dynamic mode, tabu search (37 pages, 2006)
105. Th. Hanne
Applying multiobjective evolutionary algorithms in industrial projects
Keywords: multiobjective evolutionary algorithms, discrete optimization, continuous optimization, electronic circuit design, semi-infinite programming, scheduling (18 pages, 2006)
106. J. Franke, S. Halim
Wild bootstrap tests for comparing signals and images
Keywords: wild bootstrap test, texture classification, textile quality control, defect detection, kernel estimate, nonparametric regression (13 pages, 2007)
107. Z. Drezner, S. Nickel
Solving the ordered one-median problem in the plane
Keywords: planar location, global optimization, ordered median, big triangle small triangle method, bounds, numerical experiments (21 pages, 2007)
108. Th. Götz, A. Klar, A. Unterreiter, R. Wegener
Numerical evidence for the non-existing of solutions of the equations describing rotational fiber spinning
Keywords: rotational fiber spinning, viscous fibers, boundary value problem, existence of solutions (11 pages, 2007)
109. Ph. Süß, K.-H. Küfer
Smooth intensity maps and the Bortfeld-Boyer sequencer
Keywords: probabilistic analysis, intensity modulated radiotherapy treatment (IMRT), IMRT plan application, step-and-shoot sequencing (8 pages, 2007)
110. E. Ivanov, O. Gluchshenko, H. Andrä, A. Kudryavtsev
Parallel software tool for decomposing and meshing of 3d structures
Keywords: a-priori domain decomposition, unstructured grid, Delaunay mesh generation (14 pages, 2007)
111. O. Iliev, R. Lazarov, J. Willems
Numerical study of two-grid preconditioners for 1d elliptic problems with highly oscillating discontinuous coefficients
Keywords: two-grid algorithm, oscillating coefficients, preconditioner (20 pages, 2007)
112. L. Bonilla, T. Götz, A. Klar, N. Marheineke, R. Wegener
Hydrodynamic limit of the Fokker-Planck equation describing fiber lay-down processes
Keywords: stochastic differential equations, Fokker-Planck equation, asymptotic expansion, Ornstein-Uhlenbeck process (17 pages, 2007)
113. S. Rief
Modeling and simulation of the pressing section of a paper machine
Keywords: paper machine, computational fluid dynamics, porous media (41 pages, 2007)
114. R. Ciegis, O. Iliev, Z. Lakdawala
On parallel numerical algorithms for simulating industrial filtration problems
Keywords: Navier-Stokes-Brinkmann equations, finite volume discretization method, SIMPLE, parallel computing, data decomposition method (24 pages, 2007)
115. N. Marheineke, R. Wegener
Dynamics of curved viscous fibers with surface tension
Keywords: Slender body theory, curved viscous fibers with surface tension, free boundary value problem (25 pages, 2007)